tic markers and as possible therapeutic targets as the number of trials grows for biospecific inhibitors. The *ERBB2* (also called HER-2) protooncogene, which is located on human chromosome 17, encodes a 185-kilodalton transmembrane glycoprotein that shows significant structural similarity[3] and functional association to the epidermal growth factor receptor (EGFR).[4-6] *ERBB2* has been found to be overexpressed in many different types of human malignancies, notably, lung,[7] breast,[8] ovarian,[9] pancreatic,[10] and osteosarcoma.[11,12] Overexpression of *ERBB2* in breast carcinoma has been associated with poor overall survival and has been shown to enhance malignancy and metastatic potential. Trastuzumab (Herceptin; Genentech, South San Francisco, CA), a monoclonal antibody that targets *ERBB2*, demonstrated therapeutic benefit in advanced breast carcinoma patients.[13] Aberrant expression and activation of EGFR is characteristic of many human cancers and is often associated with poor clinical outcome and chemoresistance.[14] Gefitinib (Iressa; AstraZeneca Plc., London, UK), a small molecule inhibitor of EGFR tyrosine kinase activity, has already been approved for cancer treatment.[15]

KIT, an RTK for the stem cell factor, has been implicated in the pathophysiologic mechanisms of a variety of human tumors.[16-19] Activating mutations of *KIT* have been described in gastrointestinal stromal tumors (GIST). STI571 (Glivec; Novartis Ag, Basel, Switzerland), a specific inhibitor of tyrosine kinases, has shown promise in the management of patients with GIST.[20]

Relatively little is known about expression of these RTKs in STS and their clinical significance to STS has been poorly investigated. Our group studied expression patterns of EGFR, *ERBB2*, and *KIT* on 281 patients with common adult STS by standard immunohistochemical staining and, then, verified whether a significant association with prognosis was present.

MATERIALS AND METHODS

Patients

Records of 281 patients with primary localized STSs of the extremity and trunk wall, who were diagnosed and treated between January, 1975 and December, 2002 were retrieved from the pathology files of the National Cancer Center (NCC), Tokyo, Japan. Common histologic categories such as liposarcoma, myxofibrosarcoma, malignant fibrous histiocytoma (MFH), synovial sarcoma, and spindle cell sarcoma (fibrosarcoma, leiomyosarcoma, and malignant peripheral nerve sheath tumor: MPNST) were included in the current study. MFH lesions were subdivided into pleomorphic MFH (PMFH) and myxofibrosarcoma. Liposarcoma was subclassified into well differentiated liposarcoma and myxoid liposarcoma. Dedifferentiated liposarcoma and pleomorphic liposarcoma were not included in the current study. Between the two dates, 745 newly diagnosed STS patients were seen. Among them, 379 were excluded because of tumor histology: rhabdomyosarcoma (194), alveolar soft part sarcoma (20), angiosarcoma (30), epithelioid sarcoma (25), extraskeletal myxoid chondrosarcoma (20), extraskeletal Ewing sarcoma (21), extraskeletal osteosarcoma (13), clear cell sarcoma (16), dedifferentiated liposarcoma (34) and pleomorphic liposarcoma (6). Our group excluded rhabdomyosarcoma and Ewing sarcoma, as their treatment is different. The other histologic categories were excluded because of rarity. Because tumors having the same histology will exhibit different behavior patterns depending on anatomical site,[2] 42 patients with retroperitoneal, head and neck, visceral, and intrathoracic tumors were excluded. Patients with Stage IV sarcomas (43) were also excluded.

There were 152 females and 129 males, whose ages ranged from 10 to 85 years (median 50 yrs). The clinical details, including follow-up information, were obtained by reviewing all medical charts. All of the patients underwent tumor resection. Adjuvant treatment in the form of radiotherapy (25 patients), chemotherapy (37), or both (23) was administered as part of standard care or as part of clinical trials. Preoperative adjuvant treatment was given to 43 patients. No patients were lost to follow up. Follow-up data began on the date of diagnosis. Median follow up was 60 months. Overall survival was recorded as the time to death due to cause related with disease.

The protocol of this study was reviewed and approved by the Institutional Review Board of the NCC.

Pathology Reviewing, Grade, and Staging

Histologic slides of primary tumors from all patients were reviewed for diagnosis by an NCC pathologist (T. H.) who had developed the grading system.[21] Whenever necessary, immunohistochemistry was used for confirming the diagnosis or tumor typing according to the World Health Organization Classification of Soft Tissue Tumors (2002).[22] The histologic grade is a three-grade system (using scores 0, 1, 2, 3) that is obtained by adding scores for tumor differentiation, tumor necrosis, and the MIB-1 labeling index. MIB-1 scores were determined by staining sections with an antibody for MIB-1 (1:100, Immunotech, Marseille, France). An MIB-1 score of 1 was assigned to lesions with an MIB-1 labeling index (LI) of 0–9%, an MIB-1 score of 2 was assigned to lesions with an MIB-1 LI of 10–29%, and an MIB-1 score of 3 was assigned to lesions with an MIB-1 LI $\geq$ 30%.[23] Our

TABLE 1
Primary Antibodies.

Antibody	Source	Clone	Dilution	Positive control
EGFR, mouse monoclonal	DakoCytomation[a]	2-18C9	Prediluted	Breast carcinoma
ERBB2, rabbit polyclonal	DakoCytomation		1:500	Breast carcinoma
KIT, rabbit polyclonal	DakoCytomation		1:50	Mast cells

[a] Manufacturer is located in Glostrup, Denmark.

group has previously shown that validity and reproducibility of the MIB-1 score are superior to those of the mitotic score.[24]

For TNM staging classification,[22] Grade 1 tumors that were assessed by using the above-mentioned grading system were grouped as low grade, and Grade 2 and 3 tumors as high grade. To define depth, superficial lesions did not involve the superficial fascia, and deep lesions had reached to or invaded the superficial fascia.

Immunohistochemical Analysis of EGFR, *ERBB2*, and *KIT* in Tissue Samples

Immunohistochemical analysis of *ERBB2* and *KIT* was performed on tissue sections from paraffin blocks by the labeled streptavidin-biotin method. Sections were dewaxed, rehydrated, and moistened with phosphate-buffered saline (PBS; pH 7.4). They were pretreated in an autoclave at 121 °C for 10 minutes in 10 mmol/L citrate buffer (pH 6.0), before being incubated either with antihuman *ERBB2* or *KIT* antibody on an automated immunostaining system (i6000™; BioGenex, San Ramon, CA) for 30 minutes. Immunohistochemical staining of EGFR on sections from paraffin blocks was performed according to manufacturer's instructions included with the EGFR detection system (EGFR pharmDx *kit*, DakoCytomation, Glostrup, Denmark). Specifications of primary antibodies are listed in Table 1. Anti-EGFR monoclonal antibody, clone 2-18C9, which binds to an epitope located near the ligand binding domain on the extracellular domain of EGFR, is specific for EGFR and does not crossreact with *ERBB2* or the other receptors of the *ERBB* family.[25]

In an attempt to elucidate whether the overexpressed EGFR was really functioning, immunohistochemical analysis of phosphorylated EGFR was performed on formalin-fixed, paraffin-embedded tissue sections from 20 synovial sarcomas in which an increased level of EGFR was detected. Our group used a mouse monoclonal anti-HER1pY1092 (1068) antibody, kindly provided by DakoCytomation A/S (Glostrup, Denmark), which detects specifically the levels of phosphorylated EGFR at tyrosine 1068. It does not detect other phosphorylated EGFR families.

A multiheaded microscope was used to read immunohistochemical results, which were judged by investigators, all of whom were blinded to the clinical status of patients. A consensus judgment was adopted as to the proper immunohistochemical score of a tumor based on strength: 0 = negative; 1+ = weak staining; 2+ = moderate staining; 3+ = strong staining. Negative controls, in which the primary antibody was omitted, were included with each run. Breast carcinomas with stain results of 3+ were used as positive controls for anti-EGFR and anti-*ERBB2* antibodies. Tissue mast cells, which stained a 3+ score, were used as internal positive controls for the anti-*KIT* antibody. The distribution of positive cells was also recorded to impart the diffuse or focal nature of positive cells; sporadic (positive cells < 10%); focal (11% < positive cells < 50%); diffuse (positive cells ≥ 50%). The immunohistochemical scores of 2+ and 3+ with focal to diffuse distribution were considered to be positive for all three antibodies.

Statistical Methods

The chi-square test was used to evaluate the association between two dichotomous variables. Kaplan–Meier plots and the log-rank test were used to evaluate the association of overexpression of EGFR with overall survival. Cox proportional-hazards regression analysis with forward selection of variables was performed to estimate the rate ratios for possible risk factors for the occurrence of adverse events. Data analysis was performed with an SAS software statistical package (version 6.0, SAS Institute, Cary, NC).

RESULTS

The study group comprised 281 primary STSs, which included 52 myxoid liposarcomas, 50 well differentiated liposarcomas, 53 myxofibrosarcomas, 44 PMFHs, 42 synovial sarcomas, 18 MPNTs, 11 fibrosarcomas, and 11 leiomyosarcomas.

Results are summarized in Table 2. Moderate (2+) to strong (3+) staining of EGFR was observed 168 of 281 (60%) patients, which included 39 of 44 (89%) PMFH, 47 of 53 (89%) myxofibrosarcomas, 32 of 42 (76%) synovial sarcomas, 16 of 18 (94%) MPNST, and 8 of 11 (73%) leiomyosarcomas (Figs. 1 and 2). The incidence of positive staining was lower in fibrosarcomas (4 of 11, 36%), myxoid liposarcomas (3 of 52, 6%), and well differentiated liposarcomas (19 of 50, 38%).

Overexpression of both *ERBB2* and *KIT* was limited. Moderate (2+) staining of *ERBB2* was observed in 3 synovial sarcomas, whereas weak (1+) staining was

TABLE 2
Immunohistochemical Pattern of EGFR, *ERBB2*, and *KIT* in 281 STS Patients

Histologic type	No. Patients	EGFR				*ERBB2*				*KIT*			
		0	1+	2+	3+	0	1+	2+	3+	0	1+	2+	3+
Fibrosarcoma	11	7	0	4	0	11	0	0	0	11	0	0	0
Leiomyosarcoma	11	3	0	8	0	11	0	0	0	8	3	0	0
Myxoid lipsarcoma	52	48	1	3	0	52	0	0	0	52	0	0	0
Well differentiated liposarcoma	50	28	3	11	8	50	0	0	0	50	0	0	0
Myxofibrosarcoma	53	5	0	26[a]	22	53	0	0	0	52	1	0	0
MPNST	18	1	0	6[a]	11	17	1	0	0	17	1	0	0
PMFH	44	4	0	22[a]	18	44	0	0	0	44	0	0	0
Synovial sarcoma	42	4	6	15	17	23	16	3	0	40	0	2	0
Biphasic type	11												
Spindle cells		0	2	4	5	2	9	0	0	11	0	0	0
Epithelioid cells		5	6	0	0	2	6	3	0	11	0	0	0
Monophasic type	31												
Spindle cells		4	4	11	12	21	10	0	0	29	0	2	0

MPNST: malignant peripheral nerve sheath tumor, PMFH: pleomorphic MFH.
[a] Each of these groups includes a case with sporadic distribution. They were evaluated as negative staining.

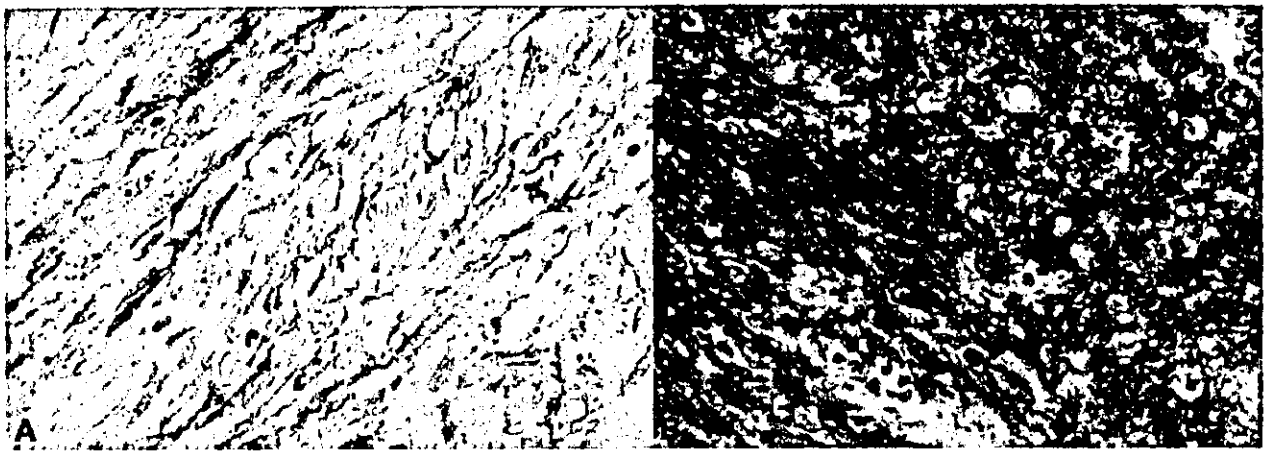

FIGURE 1. Immunohistochemical pattern of EGFR overexpression in adult soft tissue sarcoma. Moderate (2 +) and diffuse staining in a leiomyosarcoma (A), and strong (3 +) and diffuse staining in a malignant peripheral nerve sheath tumor. (Magnification × 400).

noted in 16 synovial sarcomas and 1 MPNST. In synovial sarcomas, *ERBB2* was expressed in the glandular epithelial component of 9 biphasic tumors and in solid spindle cell areas of 10 monophasic tumors. In contrast, moderate (2+) to strong (3+) staining of EGFR was found only in spindle cells of either biphasic or monophasic tumors (Fig. 2). In *KIT* expression, moderate (2+) staining was identified in 2 monophasic synovial sarcomas. Weak (1+) staining was observed in 3 leiomyosarcomas, 1 myxofibrosarcoma, and 1 MPNST

Noteworthy is that overexpressed EGFR may actually be functioning in tumors. Immunohistochemical analysis of phosphorylated EGFR was performed in 20 synovial sarcomas in which overexpression of EGFR was identified. Positive membranous staining of phosphorylated EGFR was found in 10 of 20 (50%) tumors (Fig. 3). Phosphorylated EGFR was expressed in either spindle cells or epithelioid cells of monophasic and biphasic tumors.

Association of EGFR Overexpression with Clinical and Pathologic Features

Immunostaining for EGFR was positive more frequently in superficial tumors ($P = 0.001$) and in smaller tumors ($P = 0.002$). Overexpression of EGFR was significantly associated with tumor stage and histologic grade ($P < 0.001$). No significant association

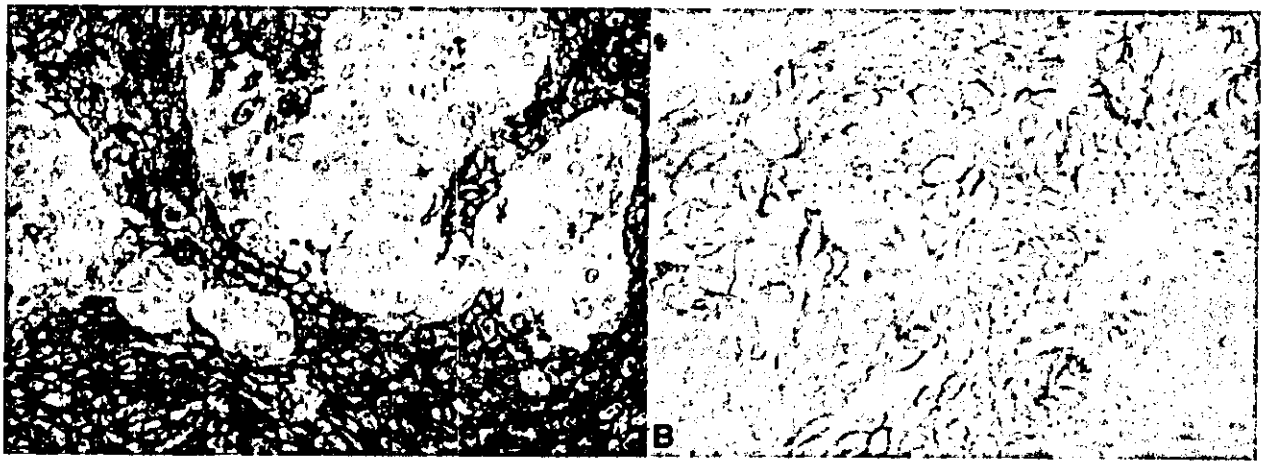

FIGURE 2. Immunohistochemical pattern of EGFR and *ERBB2* expression in a biphasic synovial sarcoma. Strong (3 +) staining of EGFR in spindle cells (A) and moderate (2 +) staining of *ERBB2* in epithelioid cells (B). (Magnification × 400).

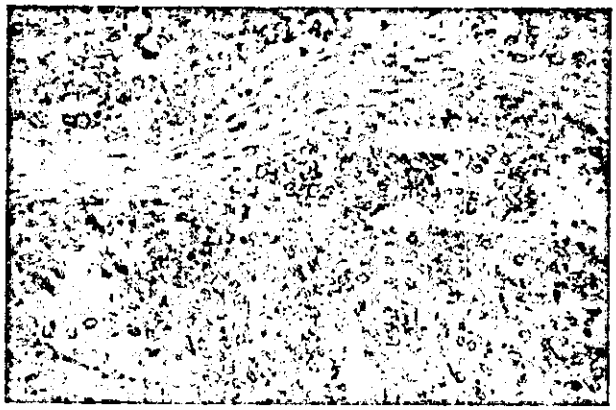

FIGURE 3. Immunohistochemical pattern of phosphorylated EGFR in synovial sarcoma in which increased levels of EGFR were detected. Positive membranous staining of phosphorylated EGFR in both epithelioid and spindle cells of a biphasic synovial sarcoma. (Magnification × 400).

was found between the incidence of EGFR positivity and age, gender, or anatomic site (Table 3).

In 281 patients, increased levels of EGFR were significantly associated with a decreased probability of overall survival ($P = 0.01$); probability of overall survival at 5 years was 63.6% in patients with increased levels of EGFR and 79.1% in patients without such overexpression (Fig. 4). The survival of these patients within each histologic subgroup was no different between EGFR positive and negative tumors (data not shown).

Several variables were tested to assess whether they had an impact on survival. Univariate analysis showed that tumor stage, histologic grade, tumor depth, tumor size, and positive EGFR staining were predictors of survival (Table 4). Multivariate analysis revealed that histologic grade and tumor size persisted as independent risk factors for poor outcome. The association between EGFR overexpression and decreased survival of patients was no longer statistically significant (Table 5). This allowed comparison between EGFR positive and negative tumors stratified either by histologic grade or tumor size (Figs. 5 and 6). There was no statistical difference in survival of patients between EGFR positive and negative tumors within each histologic grade subgroup. A significant association between EGFR overexpression and decreased survival was observed only in the > 5 cm to 10cm tumor size subgroup.

DISCUSSION

The current study provides the first immunohistochemical evidence based on large series that EGFR overexpression occurs in 60% of STSs. Increased levels of EGFR were significantly associated with a decreased overall survival on univariate analysis and correlated with histologic grade, which is an independent risk factor for a poor outcome. Moreover, phosphorylation of EGFR at tyrosine 1068 was detected in at least 50% of synovial sarcomas that overexpressed EGFR. Tyrosine 1068 within the cytoplasmic domain of the receptor is an autophosphorylation site used as a marker of receptor activation.[26] Our results indicate that this parameter may provide prognostic information and, therefore, the authors of the current study suggest that specific therapy with humanized monoclonal antibodies against EGFR or small molecular inhibitors for tyrosine kinase of EGFR be considered in a significant number of STSs. In contrast, the distribution of *ERBB2* and *KIT* overexpression is limited,

TABLE 3
Association of EGFR and Clinical Variables

Variable	No. of patients	EGFR overexpression			
		Negative	Positive	%[a]	*P* value
Age (yrs)					
< 50	123	54	69	56	0.3
≥ 50	158	59	99	63	
Gender					
Male	129	47	82	64	0.3
Female	152	66	86	57	
Site					
Extremity	202	87	115	57	0.1
Trunk	79	26	53	67	
Size					
≤ 5 cm	69	17	52	75	0.002
5–10 cm	135	55	80	59	
> 10 cm	77	41	36	47	
Tumor depth					
Superficial	65	15	50	77	0.001
Deep	216	98	118	55	
Histologic type					
Well differentiated liposarcoma	50	31	19	38	< 0.001
Myxoid liposarcoma	52	49	3	6	
Myxofibrosarcoma	53	6	47	89	
PMFH	44	5	39	89	
Synovial sarcoma	42	10	32	76	
MPNST	18	2	16	89	
Leiomyosarcoma	11	3	8	73	
Fibrosarcoma	11	7	4	36	
Histologic grade					
I	96	65	31	32	< 0.001
II	74	22	52	70	
III	111	26	85	77	
Stage					
I	72	23	49	68	< 0.001
II	129	68	61	47	
III	80	22	58	73	

PMFH: pleomorphic MFH; MPNST: malignant peripheral nerve sheath tumor.
[a] Percentage of positive cases.

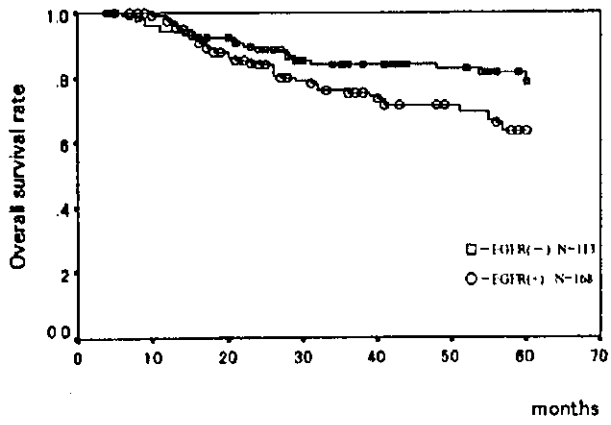

FIGURE 4. Kaplan–Meier plots for overall survival for EGFR positive cases compared with negative cases.

TABLE 4
Variables Associated with Patient Survival: Univariate Analysis

Variables	No. patie	5-yr survival rate (95% CI)	Log rank *P* value	Relative risk
Age (yrs)				
[a]< 50	123	71.0 (61.6–80.3)	0.5	(—)
≥ 50	158	69.8 (61.2–78.3)		
Gender				
Male	129	71.7 (63.4–80.1)	0.9	(—)
Female	152	71.4 (62.3–80.5)		
Site				
Extremity	202	72.1 (64.7–79.6)	0.5	(—)
Trunk	79	66.3 (54.6–78.1)		
Size				
< 5 cm	69	81.5 (70.3–91.8)	0.02	1
5–10 cm	135	71.2 (62.0–80.3)		1.8 (0.9–3.7)
> 10 cm	77	58.5 (45.4–71.5)		2.7 (1.3–5.7)
Tumor depth				
Superficial	65	81.8 (70.7–92.9)	0.04	1
Deep	216	66.8 (59.4–74.2)		2.0 (1.0–4.1)
Histologic type				
Well differentiated liposarcoma	50	100	< 0.001	(—)
Myxoid liposarcoma	52	76.7 (63.8–89.6)		
Myxofibrosarcoma	53	84.7 (73.0–96.4)		
PMFH	44	44.9 (27.5–62.3)		
Synovial sarcoma	42	58.5 (41.9–74.9)		
MPNST	18	48.2 (22.8–73.6)		
Leiomyosarcoma	11	45.5 (8.1–82.8)		
Fibrosarcoma	11	68.6 (32.1–100)		
Histologic grade				
I	96	97.8 (93.6–100)	< 0.001	1
II	74	79.7 (69.3–90.1)		13 (1.8–104)
III	111	41.9 (30.9–53.0)		57 (8.0–414)
Stage				
I	72	94.0 (87.2–100)	< 0.001	1
II	129	74.6 (65.5–83.8)		5.3 (1.6–17)
III	80	41.2 (28.2–54.2)		18 (5.4–57)
EGFR overexpression				
Negative	113	79.1 (70.5–87.6)	0.01	1
Positive	168	63.6 (54.7–72.4)		1.8 (1.1–3.0)

CI: confidence interval; PMFH: pleomorphic MFH; MPNST: malignant peripheral nerve sheath tumor.

suggesting that their therapeutic use does not appear promising.

Immunohistochemistry (IHC) is the most common method for detection of RTK overexpression, but it is significantly affected by the sensitivity and specificity of the antibodies used, the type of tissue (frozen versus formalin-fixed, paraffin-embedded), and various interpretative criteria and scoring systems used to evaluate cases. For these reasons, our group used an EGFR IHC test developed by DakoCytomation (Glostrup, Denmark), the pharm Dx EGFR IHC assay, to evaluate EGFR immunoreactivity and two polyclonal antibodies to evaluate *ERBB2* and *KIT*, respectively. These antibodies are arguably the most diffuse

TABLE 5
Factors Relevant for Survival: Cox Proportional Hazards Regression Model

Variable	Hazard ratio	95% CI	*P* value
Tumor size			
≤ 5 cm	1		
5–10 cm	1.4	0.68–3.0	0.35
> 10 cm	2.4	1.1–5.2	0.029
Depth			
Superficial	1		
Deep	1.1	0.53–2.4	0.78
Grade			
I	1		
II	16	2.2–130	0.007
III	64	8.7–480	< 0.001
EGFR overexpression			
Negative	1		
Positive	0.83	0.48–1.4	0.51

CI: confidence interval.

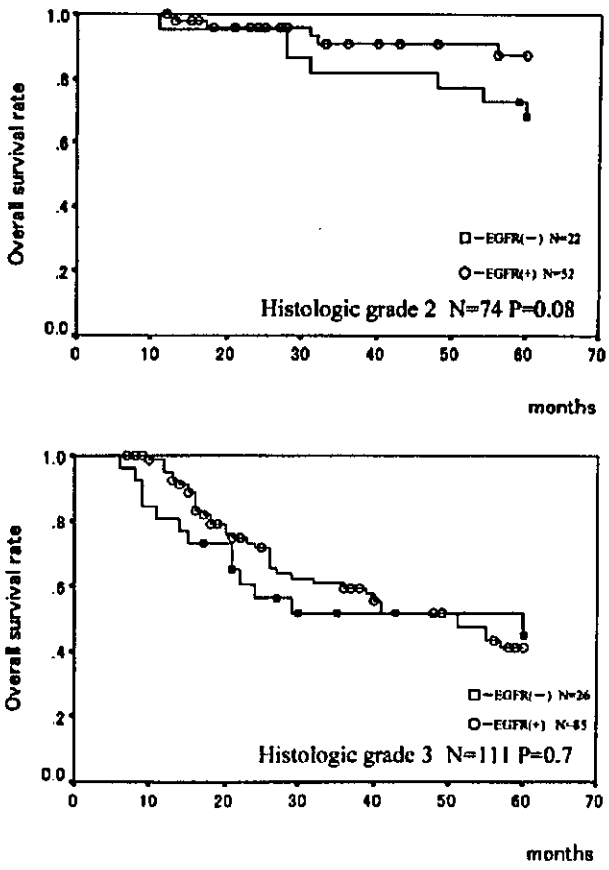

FIGURE 5. Kaplan–Meier survival curves stratified by EGFR status and by histologic grade. A: histologic Grade 2, B: histologic Grade 3

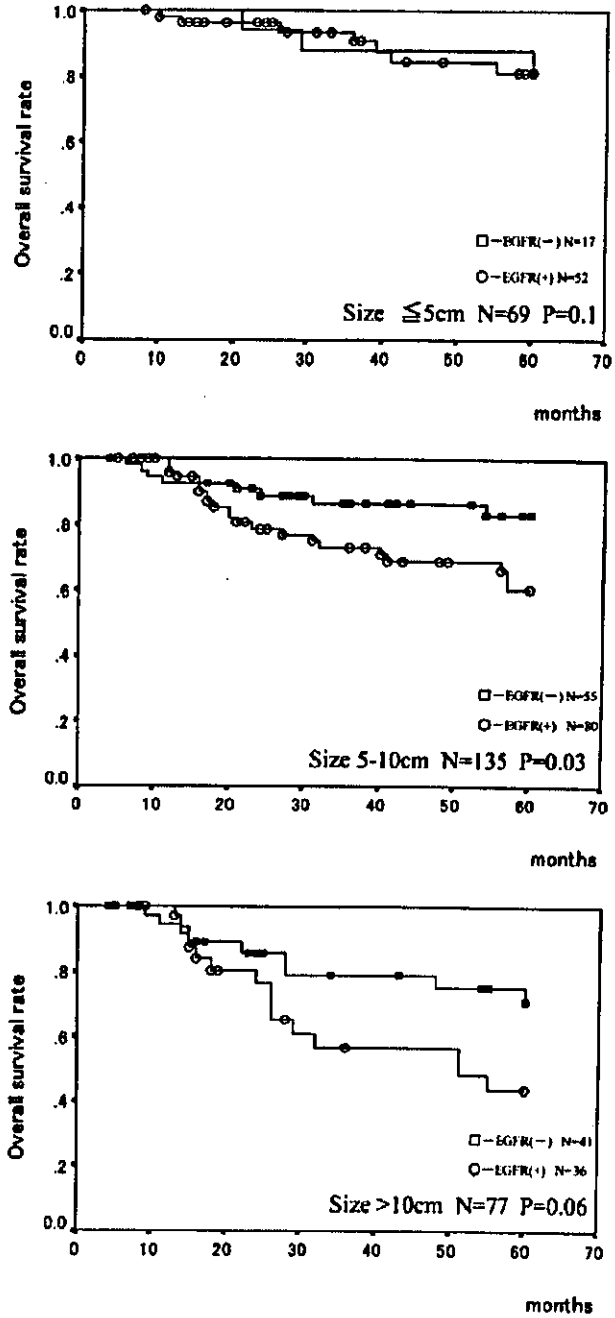

FIGURE 6. Kaplan–Meier survival curves stratified by EGFR status and by tumor size. A: size ≤ 5 cm, B: 5–10 cm, C: > 10 cm.

and thoroughly tested antibodies for each of the three RTKs. Positivity was determined by evaluating both intensity and distribution of immunostaining. The scoring system was adopted from tests of *ERBB2* expression. Breast carcinomas with stain 3+ were used as a positive control of EGFR, and *ERBB2* expression and tissue mast cells with stain 3+ were

used as an internal positive control of *KIT* expression.

The overexpression of EGFR in STSs was first documented by two teams of investigators in the 1980s. Guesterson et al.[27] identified overexpressed EGFR in 18 of 35 sarcoma specimens by IHC. Strong immunostaining was noted in MFH, epithelioid sarcoma, and synovial sarcoma. Perosio et al.[28] demonstrated that 20 of 40 STSs exhibited positive immunoreactivity. Afterward, Duda et al.[29] determined gene amplification and expression of EGFR in sarcomas. Amplification of EGFR was identified in 2 of 117 (1.7%) sarcomas. Overexpression of EGFR was identified in 21 of 43 (49%) sarcomas. The overexpression was frequently observed in MFH and leiomyosarcoma. A recent investigation reported gene expression profiles of 41 soft tissue tumors with cDNA microarray analysis. Among these sarcomas, 6 monophasic synovial sarcomas were characterized by a unique expression pattern of a cluster of 104 genes, including EGFR.[30] Barbashina et al.[31] reported that 13 of 19 (68%) synovial sarcomas were immunoreactive to EGFR. Nielsen et al.[32] showed that 52% of synovial sarcomas were strongly immunoreactive to the same monoclonal antibody, 2-18C9, used in this study. The current study expands upon previous work by demonstrating, in a larger cohort of patients, that positive staining of EGFR was found in 60% of 281 adult STSs, and that PMFH, myxofibrosarcoma, synovial sarcoma, MPNST, and leiomyosarcoma had a substantial proportion of tumors with strong, diffuse positivity for EGFR. FISH analysis, used in the current study, has also disclosed that this overexpression is not associated with gene amplification in most of the EGFR 3+ tumors (data not shown).

To date, there has been no report showing the association of EGFR overexpression and clinical outcome in STSs. In our STS patients, increased levels of EGFR were significantly associated with decreased overall survival rate, although at least by univariate analysis. When histologic grade and tumor size variables were analyzed by the Cox proportional hazards model, this association was no longer statistically significant. The stratified log-rank test failed to show statistical difference in survival of patients between EGFR positive and negative tumors in each grade–size subgroup, with the exception of the > 5–10 cm tumor size subgroup. These observations suggest that EGFR overexpression is an unfavorable prognostic factor that may have a strong association with histologic grade. The initial univariate association may be a reflection of differences in histologic grade.

Whether *ERBB2* and *KIT* overexpression occur in STSs remains controversial. Reports demonstrated that *ERBB2* is overexpressed in 30–50% of STSs.[29,31,33,34] However, Merimsky et al.[35] found no overexpression of *ERBB2* in 230 cases of STS. There have been several reports of *KIT* immunostaining in a limited number of STSs, other than GISTs, including clear cell sarcoma, synovial sarcoma, dermatofibrosarcoma protuberans, and Ewing sarcoma.[36] Hornick et al.[37] evaluated 365 specimens of STSs and found *KIT* overexpression in a very limited number of tumors. Our results are consistent with studies based on large series showing limited expression of *ERBB2* and *KIT* in STS.

There was a significant difference in EGFR expression between well differentiated and myxoid liposarcomas. It is suggested that well differentiated liposarcomas contain exclusively fibroblastic spindle and satellite cells.[38,39] In contrast, myxoid liposarcomas are neoplasms composed primarily of a mixture of cell types, varying from undifferentiated mesenchymal cells to late lipoblasts, and, occasionally, mature adipocytes.[40] The distinct tumor cell components may explain the differences in EGFR expression between these two subgroups of liposarcoma.

The overexpression of EGFR was more frequent in small and/or superficial tumors compared to large/deep tumors. There was also a significant correlation with decreased overall survival. This counterintuitive result may be explained by the heterogeneity of these groups and does not appear biologically significant. A number of small/superficial tumors included PMFH, synovial sarcomas, and MPNST, which were of high grade and expressed EGFR frequently. Conversely, a number of large/deep tumors included well differentiated liposarcomas and myxoid liposarcomas, which were of low grade and expressed EGFR less frequently.

It is unknown why tumors associated with Stage II disease were less likely to demonstrate EGFR overexpression than Stage I or III tumors. Stages are determined by histologic grade, tumor size, and tumor depth. The impact of EGFR overexpression varies according to each of the three factors, and, overall, this averaged difference is not so great. Therefore, this may be an example of random variation.

An interesting observation is reciprocal expression of EGFR and *ERBB2* in synovial sarcoma. EGFR was predominantly expressed in spindle cells, whereas *ERBB2* was expressed in epithelioid cells, which is concordant with recent studies.[31,41,42] It is likely that biphasic synovial sarcomas coexpress EGFR and *ERBB2*. *ERBB2* forms heterodimers with EGFR and modulates EGFR function.[4,5] The heterodimerization of EGFR and *ERBB2* may play a role in the mesenchymal to epithelial differentiation of synovial sarcoma. Synovial sarcoma consistently shows a specific t(X;18; p11;q11), which usually represents either of two gene fusions, SYT-SSX1 or SYT-SSX2, encoding putative

transcriptional protein differing at the 13 amino acid position. There is a strong association of fusion type and morphology, with almost all SYT-SSX2 tumors showing absence of glandular differentiation (monophasic histology) and almost all biphasic tumors containing SYT-SSX1.[43,44] It is unknown whether these translocation-derived chimeric transcription factors are associated with the *ERBB2* gene expression profile.

Therapeutic approaches targeting the EGFR signaling pathway, either alone or in combination with radiation or cytotoxic agents, are being intensively investigated. Strategies that are in various stages of development include blockade of the extracellular receptor domain,[45,46] inhibition of the intracellular tyrosine kinase activity, inhibition of receptor production by antisense approaches, expression of a truncated dominant-negative EGFR mutant, and so on. For example, anti-EGFR monoclonal antibody, IMC-C225/cetuximab, in combination with chemotherapy or radiation, is being addressed in Phase III clinical trials, and many small-molecule tyrosine kinase inhibitors are in Phase I–II clinical testing (See Grunwald.[15]). These results, along with the determination of the high frequency of EGFR expression in STS and its association with a negative prognosis, may open the door to a clinical trial of currently available biospecific inhibitors of EGFR in STS.

REFERENCES

1. Antman KH. Adjuvant therapy of sarcomas of soft tissue. *Semin Oncol.* 1997;24:556–560.
2. Stojadinovic A, Leung DH, Allen P, Lewis JJ, Jaques DP, Brennan MF. Primary adult soft tissue sarcoma: time-dependent influence of prognostic variables. *J Clin Oncol.* 2002;20:4344–4352.
3. Bargmann CI, Hung MC, Weinberg RA. The neu oncogene encodes an epidermal growth factor receptor-related protein. *Nature.* 1986;319:226–230.
4. Kokai Y, Myers JN, Wada T, Brown VI, LeVea CM, Davis JG, et al. Synergistic interaction of p185c-neu and the EGF receptor leads to transformation of rodent fibroblasts. *Cell.* 1989;58:287–292.
5. Wada T, Qian XL, Greene MI. Intermolecular association of the p185neu protein and EGF receptor modulates EGF receptor function. *Cell.* 1990;61:1339–1347.
6. Wada T, Myers JN, Kokai Y, Brown VI, Hamuro J, LeVea CM, et al. Anti-receptor antibodies reverse the phenotype of cells transformed by two interacting proto-oncogene encoded receptor proteins. *Oncogene.* 1990;5:489–495.
7. Potti A, Willardson J, Forseen C, Kishor Ganti A, Koch M, Hebert B, et al. Predictive role of HER-2/neu overexpression and clinical features at initial presentation in patients with extensive stage small cell lung carcinoma. *Lung Cancer.* 2002;36:257–261.
8. Slamon DJ, Clark GM, Wong SG, Levin WJ, Ullrich A, McGuire WL. Human breast cancer: correlation of relapse and survival with amplification of the HER-2/neu oncogene. *Science.* 1987;235:177–182.
9. Slamon DJ, Godolphin W, Jones LA, Holt JA, Wong SG, Keith DE, et al. Studies of the HER-2/neu proto-oncogene in human breast and ovarian cancer. *Science.* 1989;244:707–712.
10. Dugan MC, Dergham ST, Kucway R, Singh K, Biernat L, Du W, et al. HER-2/neu expression in pancreatic adenocarcinoma: relation to tumor differentiation and survival. *Pancreas.* 1997;14:229–236.
11. Kilpatrick SE, Geisinger KR, King TS, Sciarrotta J, Ward WG, Gold SH, et al. Clinicopathologic analysis of HER-2/neu immunoexpression among various histologic subtypes and grades of osteosarcoma. *Mod Pathol.* 2001;14:1277–1283.
12. Akatsuka T, Wada T, Kokai Y, Kawaguchi S, Isu K, Yamashiro K, et al. ErbB2 expression is correlated with increased survival of patients with osteosarcoma. *Cancer* 2002;94:1397–1404.
13. Slamon DJ, Leyland-Jones B, Shak S, Fuchs H, Paton V, Bajamonde A, et al. Use of chemotherapy plus a monoclonal antibody against HER-2 for metastatic breast cancer that overexpresses HER-2. *N Engl J Med.* 2001;344:783–792.
14. Salomon DS, Brandt R, Ciardiello F, Normanno N. Epidermal growth factor-related peptides and their receptors in human malignancies. *Crit Rev Oncol Hematol.* 1995;19:183–232.
15. Grunwald V, Hidalgo M. Developing inhibitors of the epidermal growth factor receptor for cancer treatment. *J Natl Cancer Inst.* 2003;95:851–867.
16. Turner AM, Zsebo KM, Martin F, Jacobsen FW, Bennett LG, Broudy VC. Nonhematopoietic tumor cell lines express stem cell factor and display c-*kit* receptors. *Blood.* 1992;80:374–381.
17. DiPaola RS, Kuczynski WI, Onodera K, Ratajczak MZ, Hijiya N, Moore J, et al. Evidence for a functional kit receptor in melanoma, breast, and lung carcinoma cells. *Cancer Gene Ther.* 1997;4:176–182.
18. Tian Q, Frierson HF, Jr., Krystal GW, Moskaluk CA. Activating c-kit gene mutations in human germ cell tumors. *Am J Pathol.* 1999;154:1643–1647.
19. Hirota S, Isozaki K, Moriyama Y, Hashimoto K, Nishida T, Ishiguro S, et al. Gain-of-function mutations of c-kit in human gastrointestinal stromal tumors. *Science.* 1998;279:577–580.
20. Joensuu H, Roberts PJ, Sarlomo-Rikala M, Andersson LC, Tervahartiala P, Tuveson D, et al. Effect of the tyrosine kinase inhibitor STI571 in a patient with a metastatic gastrointestinal stromal tumor. *N Engl J Med.* 2001;344:1052–1056.
21. Hasegawa T, Yamamoto S, Yokoyama R, Umeda T, Matsuno Y, Hirohashi S. Prognostic significance of grading and staging systems using MIB-1 score in adult patients with soft tissue sarcoma of the extremities and trunk. *Cancer.* 2002;95:843–851.
22. Fletcher CD, Sundaram M, Rydholm A, Coindre JM, Singer S. Soft tissue tumours: epidemiology, clinical features, histological typing and grading. In: Fletcher CD, Unni KK, Mertens F, World Health Organization classification of tumours, pathology and genitics: tumors of soft tissue and bone. Lyon: IARCPress, 2002:12–18.
23. Hasegawa T, Yokoyama R, Lee YH, Shimoda T, Beppu Y, Hirohashi S. Prognostic relevance of a histological grading system using MIB-1 for adult soft-tissue sarcoma. *Oncology.* 2000;58:66–74.
24. Hasegawa T, Yamamoto S, Nojima T, Hirose T, Nikaido T, Yamashiro K, et al. Validity and reproducibility of histologic diagnosis and grading for adult soft-tissue sarcomas. *Hum Pathol.* 2002;33:111–115.

25. Spaulding DC, Spaulding BO. Epidermal growth factor receptor expression and measurement in solid tumors. *Semin Oncol.* 2002;29:45–54.
26. Nielsen UB, Cardone MH, Sinskey AJ, MacBeath G, Sorger PK. Profiling receptor tyrosine kinase activation by using Ab microarrays. *Proc Natl Acad Sci U S A.* 2003;100:9330–9335.
27. Gusterson B, Cowley G, McIlhinney J, Ozanne B, Fisher C, Reeves B. Evidence for increased epidermal growth factor receptors in human sarcomas. *Int J Cancer.* 1985;36:689–693.
28. Perosio PM, Brooks JJ. Expression of growth factors and growth factor receptors in soft tissue tumors. Implications for the autocrine hypothesis. *Lab Invest.* 1989;60:245–253.
29. Duda RB, Cundiff D, August CZ, Wagman LD, Bauer KD. Growth factor receptor and related oncogene determination in mesenchymal tumors. *Cancer.* 1993;71:3526–3530.
30. Nielsen TO, West RB, Linn SC, Alter O, Knowling MA, O'Connell JX, et al. Molecular characterisation of soft tissue tumours: a gene expression study. *Lancet.* 2002;359:1301–1307.
31. Barbashina V, Benevenia J, Aviv H, Tsai J, Patterson F, Aisner S, et al. Oncoproteins and proliferation markers in synovial sarcomas: a clinicopathologic study of 19 cases. *J Cancer Res Clin Oncol.* 2002;128:610–616.
32. Nielsen TO, Hsu FD, O'Connell JX, Gilks CB, Sorensen PH, Linn S, et al. Tissue microarray validation of epidermal growth factor receptor and SALL2 in synovial sarcoma with comparison to tumors of similar histology. *Am J Pathol.* 2003;163:1449–1456.
33. Sato T, Peiper M, Heinecke A, Zurakowski D, Eisenberger CF, Hosch S, et al. Expression of HER-2/neu Does not Correlate with Survival in Soft Tissue Sarcoma. *Onkologie.* 2003; 26:268–271.
34. Foster H, Knox S, Ganti AK, Hebert BJ, Koch M, Tendulkar K, et al. HER-2/neu overexpression detected by immunohistochemistry in soft tissue sarcomas. *Am J Clin Oncol.* 2003;26: 188–191.
35. Merimsky O, Issakov J, Schwartz I, Dadia S, Kollender Y, Bickels J, et al. Lack of ErbB-2 oncogene product overexpression in soft tissue sarcomas. *Acta Oncol.* 2002;41:366–368.
36. Smithey BE, Pappo AS, Hill DA. C-kit expression in pediatric solid tumors: a comparative immunohistochemical study. *Am J Surg Pathol.* 2002;26:486–492.
37. Hornick JL, Fletcher CD. Immunohistochemical staining for KIT (CD117) in soft tissue sarcomas is very limited in distribution. *Am J Clin Pathol.* 2002;117:188–193.
38. Bolen JW, Thorning D. Liposarcomas. A histogenetic approach to the classification of adipose tissue neoplasms. *Am J Surg Pathol.* 1984;8:3–17.
39. Chorneyko K. The ultrastructure of liposarcomas with attention to "dedifferentiation." *Ultrastruct Pathol.* 1997;21:545–557.
40. Hasegawa T, Seki K, Hasegawa F, Matsuno Y, Shimodo T, Hirose T, et al. Dedifferentiated liposarcoma of retroperitoneum and mesentery: varied growth patterns and histological grades:a clinicopathologic study of 32 cases. *Hum Pathol.* 2000;31:717–727.
41. Allander SV, Illei PB, Chen Y, Antonescu CR, Bittner M, Ladanyi M, et al. Expression profiling of synovial sarcoma by cDNA microarrays: association of ERBB2, IGFBP2, and ELF3 with epithelial differentiation. *Am J Pathol.* 2002;161:1587–1595.
42. Nuciforo PG, Pellegrini C, Fasani R, Maggioni M, Coggi G, Parafioriti A, et al. Molecular and immunohistochemical analysis of HER-2/neu oncogene in synovial sarcoma. *Hum Pathol.* 2003;34:639–645.
43. Kawai A, Woodruff J, Healey JH, Brennan MF, Antonescu CR, Ladanyi M. SYT-SSX gene fusion as a determinant of morphology and prognosis in synovial sarcoma. *N Engl J Med.* 1998;338:153–160.
44. Ladanyi M, Antonescu CR, Leung DH, Woodruff JM, Kawai A, Healey JH, et al. Impact of SYT-SSX fusion type on the clinical behavior of synovial sarcoma: a multi-institutional retrospective study of 243 patients. *Cancer Res.* 2002;62:135–140.
45. Huang SM, Harari PM. Modulation of radiation response after epidermal growth factor receptor blockade in squamous cell carcinomas: inhibition of damage repair, cell cycle kinetics, and tumor angiogenesis. *Clin Cancer Res.* 2000; 6:2166–2174.
46. Goldstein NI, Prewett M, Zuklys K, Rockwell P, Mendelsohn J. Biological efficacy of a chimeric antibody to the epidermal growth factor receptor in a human tumor xenograft model. *Clin Cancer Res.* 1995;1:1311–1318.

ELSEVIER

European Journal of Cardio-thoracic Surgery 25 (2004) 155–159

EUROPEAN JOURNAL OF CARDIO-THORACIC SURGERY

www.elsevier.com/locate/ejcts

Inflammatory myofibroblastic tumor of the lung

Hiroyuki Sakurai[a,b,*], Tadashi Hasegawa[b], Shun-ichi Watanabe[a], Kenji Suzuki[a], Hisao Asamura[a], Ryosuke Tsuchiya[a]

[a]*Division of Thoracic Surgery, National Cancer Center Hospital, 1-1, Tsukiji 5-chome, Chuo-ku, Tokyo 104-0045, Japan*
[b]*Division of Pathology, National Cancer Center Hospital, 1-1, Tsukiji 5-chome, Chuo-ku, Tokyo 104-0045, Japan*

Received 30 August 2003; received in revised form 21 October 2003; accepted 22 October 2003

Abstract

Objective: Inflammatory myofibroblastic tumor (IMT) is a rare disease that usually occurs in the lung. Recently, several reports have suggested that IMT is a true neoplasm rather than a reactive lesion. In this retrospective study, we reviewed clinicopathological characteristics and prognoses for all patients with surgically resected IMT of the lung at our institute. **Methods:** From January 1985 to December 2002, nine patients had surgical intervention for IMT of the lung at the National Cancer Center Hospital, Tokyo. The resected lesions were studied histologically, immunohistochemically, and ultrastructurally. Follow-up was complete in all patients and varied from 3 months to 16 years 2 months (median, 6 years 2 months). **Results:** These nine patients included five men and four women. They ranged in age from 25 to 66 years. Seven patients were asymptomatic. The two symptomatic patients had problems including cough, hemoptysis, and dyspnea. For all these patients, the diagnostic procedure was surgical excision. The resected tumor size ranged from 1.0 to 4.0 cm in diameter. Histologically, a variety of inflammatory and spindle cells were observed. The spindle cells corresponded ultrastructurally to myofibroblasts or fibroblasts. With the exception of one patient who had spontaneous resolution of a recurrent tumor, there was no recurrence in these patients, and all of them are in good health. **Conclusions:** Histopathologically, IMT is characterized by myofibroblasts that are mixed with chronic inflammatory cells, including plasma cells, lymphocytes, and histiocytes. Surgical resection, when possible, can be chosen as the treatment. Complete resection leads to excellent survival.

Keywords: Lung pathology; Surgery; Survival; Inflammatory pseudotumor; Pulmonary neoplasm

1. Introduction

Inflammatory myofibroblastic tumor (IMT) is a rare disease that usually occurs in the lung. IMT has been described by various terms because of its variable cellular components, which includes plasma cell granuloma, inflammatory pseudotumor, xanthogranuloma, and fibrous histiocytoma [1–18]. The notion of IMT being a reactive lesion or a neoplasm was controversial [18]. However, this entity has been characterized by not variable chronic inflammatory cells but myofibroblasts, and the recent cytogenetic studies have suggested that IMT is a true neoplasm [14–16]. There is little information on the clinicopathological features because IMT is rare and its terminology was confusing.

To examine the clinicopathological characteristics and prognosis, we reviewed a set of patients with surgically resected IMT of the lung.

2. Material and methods

2.1. Patients

Between January 1985 and December 2002, nine patients had surgical intervention for IMT of the lung at the National Cancer Center Hospital, Tokyo. These patients comprised 0.18% of 4893 patients who had thoracic surgical procedures at our institute during the same period. The clinical characteristics of these patients are shown in Table 1. Preoperative work-up included laboratory examinations, fiberoptic bronchoscopy, chest radiograph, and computed tomographic (CT) scans. Follow-up was complete in all

* Corresponding author. Tel.: +81-3-3542-2511; fax: +81-3-3542-3815.
E-mail address: sakuraihm@ybb.ne.jp (H. Sakurai).

1010-7940/$ - see front matter © 2003 Elsevier B.V. All rights reserved.
doi:10.1016/S1010-7940(03)00678-X

Table 1
Clinical characteristics of patients with inflammatory myofibroblastic tumor

Case	Sex/age	Symptom	Location	Tumor size (cm)	Mode of operation	Prognosis after surgery
1	F/59	None	HLN	2.5	Extirpation	16 years 2 months, alive
2	F/41	None	LLL	1.0	Lobectomy	13 years 9 months, alive
3	F/58	Cough/ Hemoptysis	RIB	2.0	Bilobectomy	1 year 4 months, alive
4	M/25	None	LUL	2.2	Segmentectomy	2 years 3 months, alive
5	M/49	None	LUL	3.6	Segmentectomy	9 years 6 months, alive
6	M/66	None	LUL	3.5	Segmentectomy	6 years 6 months, alive
7	M/47	Cough/ Dyspnea	LMB	4.0	Segmental bronchial resection	6 months, alive
8	M/26	None	LLL	3.0	Segmentectomy	5 years 2 months, alive
9	F/30	None	RUL	3.2	Lobectomy	3 months, alive

HLN, hilar lymph node; LLL, left lower lobe; RIB, right intermediate bronchus; LUL, left upper lobe; LMB, left main bronchus; RUL, right upper lobe.

patients and ranged from 3 months to 16 years 2 months (median, 6 years 2 months).

2.2. Pathological and ultrastructural evaluations

In each case, the tissue was fixed in 10% buffered formalin, processed routinely, and embedded in paraffin. Sections 4 μm thick, were cut and then stained with hematoxylin and eosin. Each section was also evaluated immunohistochemically. Immunohistochemical staining was accomplished by the labeled streptavidin-biotin method using an LSAB kit (Dako Corporation, Carpinteria, CA). Primary antibodies against various antigens were used in this study: vimentin (V10 clone; Dako; 1:200), cytokeratin (CAM5.2 clone; Becton Dickinson, San Jose, CA; 1:100), cytokeratin (AE1/AE3 clone; Dako; 1:125), desmin (Dako; 1:500), smooth muscle actin (1A4 clone; Dako; 1:100), CD34 (My10 clone; Becton Dickinson; 1:100), S100 protein (Dako; 1:2000), and epithelial membrane antigen (Dako; 1:100).

Small fresh fragments of tumor tissue in four cases (cases 3, 4, 7 and 9) were fixed in 2.5% glutaraldehyde, post-fixed in 1% osmium tetroxide, and embedded in epoxy resin. After contrasting with uranyl acetate and lead citrate, ultrathin sections were examined with a transmission electron microscope.

3. Results

3.1. Clinical findings

These nine patients included five men and four women. They ranged in age from 25 to 66 years, with a mean age of 44.6 years. Seven patients were asymptomatic and were found to have pulmonary nodules on routine chest radiography (Fig. 1). One of these patients (case 6) was clinically suspected of pulmonary metastasis. This was pointed out during postoperative follow-up of a right nephrectomy for renal cell carcinoma that the patient had undergone 5 years before. The two symptomatic patients had problems including cough, hemoptysis, and dyspnea. The preoperative laboratory results were within normal limits for eight patients, but one patient (case 5) had a C-reactive protein (CRP) rate of 9.4 mg/dl and a white blood cell (WBC) count of 10,000/μl. These findings returned to normal within 10 days after operation. All patients underwent a fiberoptic bronchoscopy preoperatively. Six patients did not have any bronchial abnormality. One (case 1) had a stenosis of the right basal bronchus. The other two had an endobronchial tumor. One patient (case 7) with an endobronchial tumor had complete atelectasis of the left lung (Fig. 2). Chest CT showed a solitary, well-circumscribed nodule or mass in all patients. A definitive diagnosis of IMT was not made in any of the patients, although all patients had undergone transbronchial biopsy or transthoracic needle biopsy for diagnosis preoperatively. The spindle cells and inflammatory cells in small biopsied specimen, even if they were taken by biopsy, were useless for

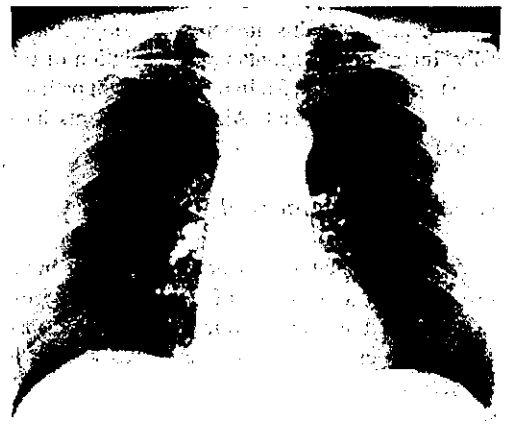

Fig. 1. Chest radiograph shows a well-defined mass in the left lung (case 5).

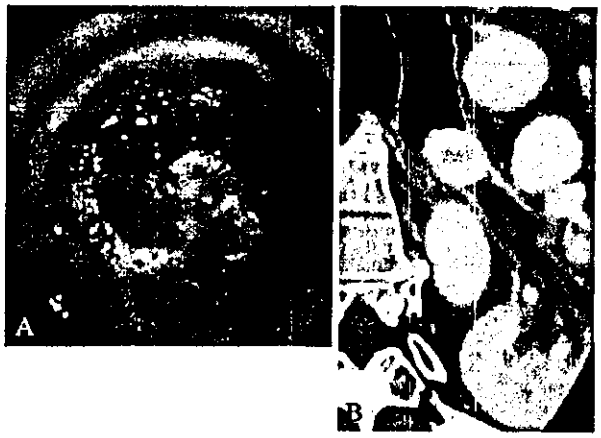

Fig. 2. This patient (case 7) had complete atelectasis of the left whole lung. Bronchoscopy shows a polypoid lesion, which almost completely occluded the left main bronchus (A). Chest CT on the coronal view shows a well-circumscribed enhanced mass with occlusion of left main bronchus (B).

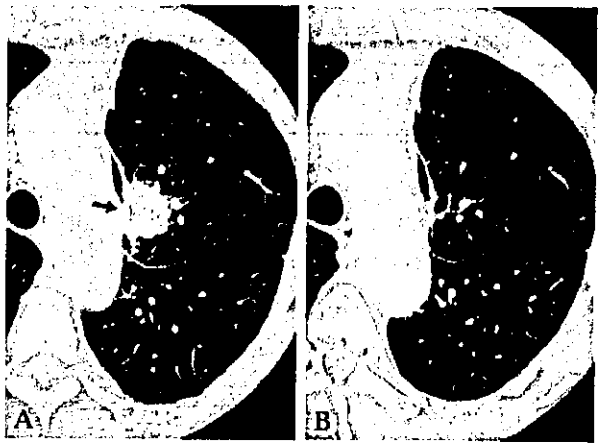

Fig. 3. On the CT findings, one patient (case 6) suffered from margin relapse, which developed adjacent to resected staple line (arrow), 4 years after initial resection (A). About 8 months later, spontaneous resolution of the tumor has been observed (B).

the definitive diagnosis because they followed a variety of lesions such as inflammation or malignancy. One patient (case 6) had an erroneous diagnosis of adenocarcinoma by aspiration cytology, because the cytologic findings showed atypical epithelial-like cells with lymphocytes and histiocytes. For all these patients, the diagnostic procedure was surgical excision. Although an intraoperative frozen section was done for the tumor in all cases, the confirmed diagnosis could not be made. However, all the tumors were regarded as low-grade malignancy because of low nuclear atypia and infrequent mitosis. The extent of surgical excision was as follows: segmentectomy in four patients, segmental bronchial resection in one, lobectomy in two, bilobectomy with bronchoplasty in one, and extirpation in one. Complete resection of the tumor was accomplished in eight patients (89%). One patient (case 7) had a pathological residual tumor in the submucosal tissue of the left main bronchus. None of the operations resulted in death. On the follow-up CT one patient (case 6) had a suspected recurrent tumor developing adjacent to the resected line four years after the initial resection, although this tumor was not evaluated histologically. Interestingly, spontaneous resolution of this tumor has been observed (Fig. 3). In the other eight patients, no recurrence of IMT occurred. All of the patients have remained healthy.

3.2. Pathological and ultrastructural findings

The resected tumor size ranged from 1.0 to 4.0 cm in the greatest diameter, with a mean of 2.8 cm. For gross appearance, most of the tumors were well-circumscribed masses without fibrous capsules and yellow to whitish in color on cut section.

Microscopically, the lesions consisted of a variety of inflammatory and mesenchymal cells, including plasma cells, histiocytes, lymphocytes, and spindle cells. All of the tumors showed interlacing fascicles, or a storiform pattern of spindle cells and an admixture of diverse inflammatory cells (Fig. 4A). The spindle cells had low cellular atypia and no mitotic activity (Fig. 4B). Blood vessel invasion was identified in one instance (case 4).

Immunohistochemically, most of spindle cells in all nine cases showed diffuse and strong reactivity for vimentin. All tumors exhibited reactivity for smooth muscle actin (Fig. 5). The staining was diffuse in eight of nine cases (89%) and focal in one (11%). One tumor exhibited focal staining for desmin. All tumors were negative for cytokeratins, CD34, S100 protein, and epithelial membrane antigen.

Ultrastructurally, two tumors (cases 3 and 9) out of four contained a varying proportion of myofibroblastic cells, as well as fibroblastic cells with a prominent Golgi apparatus

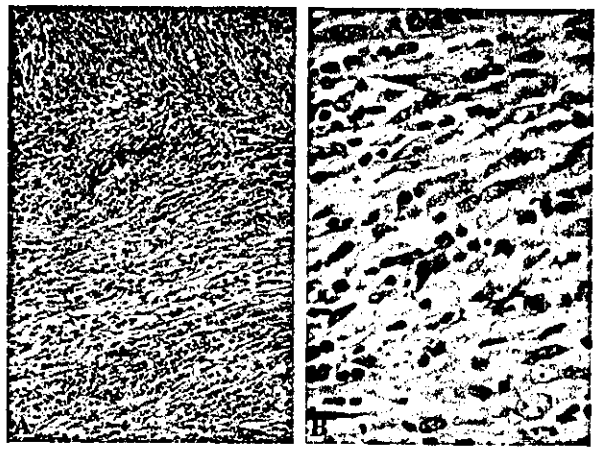

Fig. 4. Photomicrographs show an inflammatory myofibroblastic tumor. The lesion is composed of spindle cells arranged in interlacing fascicles, with admixed diverse inflammatory cells (A). The spindle cells have low cellular atypia and no mitotic activity, and the inflammatory cells are mature (B). (both, hematoxylin-eosin; A, original magnification 100 ×, B, original magnification 400 ×).

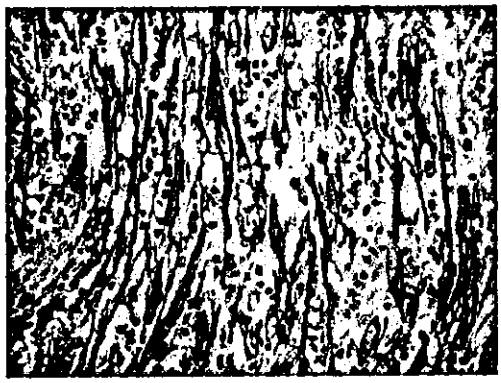

Fig. 5. Immunohistochemically, the spindle cells of the lesion show diffuse and strong reactivity for smooth muscle actin (immunohistochemistry for smooth muscle actin, original magnification 200×).

and well developed rough endoplasmic reticulum (RER). The myofibroblastic tumor cells were recognized by the presence of an often well developed branching RER and primarily peripheral bundles of actin microfilaments with interspersed fusiform densities (Fig. 6). Subplasmalemmal attachment plaques, focal basal lamina-like material, and micropinocytotic vesicles were present to variable degrees in these cells. The other tumors consisted of fibroblastic and histiocytic cells with lysosomes and lipid droplets.

4. Discussion

IMT of the lung is rare, and its incidence is reported to be 0.04–1% of all tumors of the lung [1,3]. Although IMT can grow at a wide variety of other sites [19,20], it usually arises within the lung [1]. Concerning the age of patients at diagnosis, the mean age of 44.6 years in this study was relatively older than those reported previously [4,5,7,10,17]. According to previous reports, most of the patients were

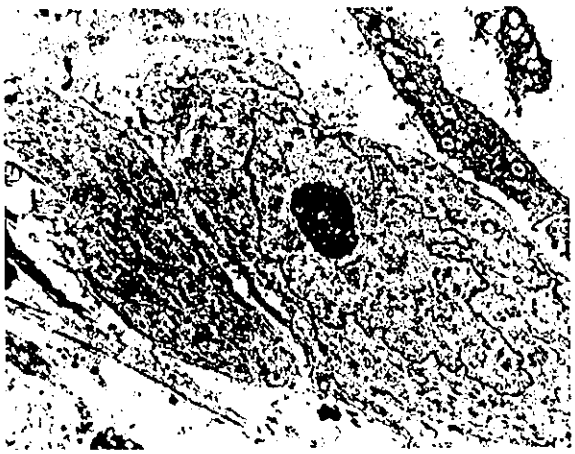

Fig. 6. Ultrastructurally, the myofibroblastic tumor cell is recognized by the presence of a well developed branching RER and primarily peripheral bundles of actin microfilaments with interspersed fusiform densities.

under 40 years old, with a mean age of 27–50 years. There was no predominance of either sex. The precise etiology of IMT of the lung is still unknown. Although a history of prior pulmonary infection in some patients with IMT has been pointed out [4], this type of patient was not found in the present study. Patients with IMT usually are asymptomatic, with a solitary nodule or mass detected by routine chest roentgenogram [5]. Endobronchial growth of IMT has only rarely been observed [2,6,7], with a prevalence of between 0 and 12%. In this study we had a relatively high prevalence (two of nine, or 22%) of patients with endobronchial growth of IMT. On the other hand, it has been known that IMT carries a risk of extension to neighboring organs [1,4,9,11], in particular to the mediastinum, although we did not observe this. Preoperative laboratory findings indicated that only one patient (11%) with a solitary pulmonary mass had an elevated CRP rate and WBC count, and the IMT appeared to have no connection with these laboratory findings [3,4]. The preoperative diagnosis of IMT is seldom confirmed, and small biopsied specimens are generally considered insufficient for diagnosis because of the predominance of inflammatory cells.

Pathologically, IMT is composed of a variable inflammatory and mesenchymal cellular mixture including plasma cells, histiocytes, lymphocytes, and spindle cells. Therefore, depending on the predominant cellular components, many synonyms for this disease have been described. In 1990, Pettinato and colleagues referred to this entity as IMT because the bulk of the lesion invariably consisted of not specific inflammatory cells, but proliferative myofibroblasts and fibroblasts [17]. Most of the spindle cells were myofibroblasts, which showed immunohistochemical staining for vimentin and smooth muscle actin, and consistent ultrastructural features. The spindle cells commonly have low cellular atypia and no mitotic activity. Inflammatory cells are mature and have no cellular atypia, and do not show monoclonal proliferation [3,17,18]. IMT occasionally invades bronchi or blood vessels [8,18]. We treated one patient (11%) with IMT who showed blood vessel invasion (case 4). However, it is doubtful that these are truly the tumor infiltrations, because the existing histologic architecture of the lung can also be destroyed by infiltration of only inflammatory cells. Furthermore, distant metastases from IMT are hardly ever reported. The differential diagnosis of IMT is multifarious because of its variable cellular admixture. It includes malignant lymphoma, lymphoid hyperplasia, pseudolymphoma, plasmacytoma, malignant fibrous histiocytoma, sarcomatoid carcinoma of the lung, sclerosing hemangioma, sarcoma, and/or nodular chronic pneumonitis. These lesions can be differentiated by careful attention to cellular atypia, necrosis, mitotic activity, immunoreactivity, or clonality [1,9,18]. IMT of the lung also has the histologic resemblance to the fibromas of the parietal or visceral pleuras. The fibromas shows short fascicles or haphazard fashion of spindle cells with few inflammatory cells, whereas IMT shows interlacing

fascicles or a storiform pattern of spindle cells and an admixture of diverse inflammatory cells [21].

Although the notion of IMT being a reactive lesion or a neoplasm had been controversial, IMT has been recently thought of as a neoplasm rather than a reactive lesion because of clonal chromosomal abnormalities [15], chromosomal rearrangements involving the ALK receptor tyrosine-kinase locus region (chromosome band 2p23) [16], or DNA aneuploidy in IMT [14]. IMT usually grows locally and slowly. Therefore, taking into account these histopathologic and biological findings, IMT may be regarded as low-grade malignancy or benign tumor.

Surgical resection is recommended as the treatment of choice. Cerfolio and colleagues reported that the residual tumor became enlarged in 60% of patients who had incomplete resection [1]. They advocated the importance of initial complete resection of the tumor. Surgical removal usually fills the role of both diagnosis and treatment. The effectiveness of radiotherapy, chemotherapy, or steroids is uncertain [1,12]. The spontaneous regression of IMT has been reported only infrequently [9]. Likewise, we cared for one patient with spontaneous regression of the recurrent tumor, although this was not confirmed histologically. The causes of these remissions are unknown. The outcome after resection is usually excellent, and all of the patients in this study have also remained well over the longer term. However, long-term follow-up is necessary because of reported cases of recurrences many years after resection [2,22].

In conclusion, IMT of the lung is rare. Histopathologically, IMT is characterized by myofibroblasts that are mixed with chronic inflammatory components, consisting of plasma cells, lymphocytes, and histiocytes. Surgical resection, when possible, is recommended as the treatment of choice. The outcome after complete resection is excellent.

References

[1] Cerfolio RJ, Allen MS, Nascimento AG, Deschamps C, Trastek VF, Miller DL, Pairolero PC. Inflammatory pseudotumors of the lung. Ann Thorac Surg 1999;67:933–6.

[2] Matsubara O, Tan-Liu NS, Kenney RM, Mark EJ. Inflammatory pseudotumors of the lung: progression from organizing pneumonia to fibrous histiocytoma or to plasma cell granuloma in 32 cases. Hum Pathol 1988;19:807–14.

[3] Ishida T, Oka T, Nishino T, Tateishi M, Mitsudomi T, Sugimachi K. Inflammatory pseudotumor of the lung in adults: radiographic and clinicopathological analysis. Ann Thorac Surg 1989;48:90–5.

[4] Berardi RS, Lee SS, Chen HP, Stines GJ. Inflammatory pseudotumors of the lung. Surg Gynecol Obstet 1983;156:89–96.

[5] Agrons GA, Rosado-de-Christenson ML, Kirejczyk WM, Conran RM, Stocker JT. Pulmonary inflammatory pseudotumor: radiologic features. Radiology 1998;206:511–8.

[6] Calderazzo M, Gallelli A, Barbieri V, Roccia F, Pelaia G, Tranfa CME, Cavaliere S, Zorzi F. Inflammatory pseudotumour of the lung presenting as an airway obstructive syndrome. Respir Med 1997;91: 381–4.

[7] Bahadori M, Liebow AA. Plasma cell granulomas of the lung. Cancer 1973;31:191–208.

[8] Warter A, Satge D, Roeslin N. Angioinvasive plasma cell granulomas of the lung. Cancer 1987;59:435–43.

[9] Mandelbaum I, Brashear RE, Hull MT. Surgical treatment and course of pulmonary pseudotumor (plasma cell granuloma). J Thorac Cardiovasc Surg 1981;82:77–82.

[10] Copin MC, Gosselin BH, Ribet ME. Plasma cell granuloma of the lung: difficulties in diagnosis and prognosis. Ann Thorac Surg 1996; 61:1477–82.

[11] Urschel JD, Horan TA, Unruh HW. Plasma cell granuloma of the lung. J Thorac Cardiovasc Surg 1992;104:870–5.

[12] Imperato JP, Folkman J, Sagerman RH, Cassady JR. Treatment of plasma cell granuloma of the lung with radiation therapy: a report two cases and a review of the literature. Cancer 1986;57:2127–9.

[13] Grossman RE, Bemis EL, Pemberton AH, Narodick BG. Fibrous histiocytoma or xanthoma of the lung with bronchial involvement. J Thorac Cardiovasc Surg 1973;65:653–7.

[14] Biselli R, Ferlini C, Fattorossi A, Boldrini R, Bosman C. Inflammatory myofibroblastic tumor (inflammatory pseudotumor): DNA flow cytometric analysis of nine pediatric cases. Cancer 1996; 77:778–84.

[15] Snyder CS, DellAquila M, Haghighi P, Baergen RN, Suh YK, Yi ES. Clonal changes in inflammatory pseudotumor of the lung: a case report. Cancer 1995;76:1545–9.

[16] Lawrence B, Perez-Atayde A, Hibbard MK, Rubin BP, Cin PD, Pinkus JL, Pinkus GS, Xiao S, Yi ES, Fletcher CD, Fletcher JA. TPM3-ALK and TPM4-ALK oncogenes in inflammatory myofibroblastic tumors. Am J Pathol 2000;157:377–84.

[17] Pettinato G, Manivel JC, De Rose N, Dehner LP. Inflammatory myofibroblastic tumor (plasma cell granuloma): clinicopathologic study of 20 cases with immunohistochemical and ultrastructural observations. Am J Clin Pathol 1990;94:538–46.

[18] Matsubara O, Mark EJ, Ritter JH. Pseudoneoplastic lesions of the lungs, pleural surfaces, and mediastinum. In: Wick MR, Humphrey PA, Ritter JH, editors. Pathology of pseudoneoplastic lesions. New York: Lippincott-Raven, Inc.; 1997. p. 100–9.

[19] Perrone T, De Wolf-Peeters C, Frizzera G. Inflammatory pseudotumor of lymph nodes: a distinctive pattern of nodal reaction. Am J Surg Pathol 1988;12:351–61.

[20] Anthony PP, Telesinghe PU. Inflammatory pseudotumor of the liver. J Clin Pathol 1986;39:761–8.

[21] Colby TV, Koss MN, Travis WD. Fibrous and fibrohistiocytic tumors and tumor-like conditions. In: Rosai J, Sobin LH, editors. Atlas of tumor pathology. 3rd series. Tumors of the lower respiratory tract, vol. 13. Washington: Armed Forces Institute of Pathology (AFIP); 1995. p. 203–34.

[22] Weinberg PB, Bromberg PA, Askin FB. Recurrence of a plasma cell granuloma 11 years after initial resection. South Med J 1987;80: 519–21.

Prognostic Significance of MRI Findings in Patients with Myxoid–Round Cell Liposarcoma

Ukihide Tateishi[1]
Tadashi Hasegawa[2]
Yasuo Beppu[3]
Akira Kawai[3]
Mitsuo Satake[1]
Noriyuki Moriyama[1]

OBJECTIVE. The aims of this study were to determine the prognostic significance of MRI findings in patients with myxoid–round cell liposarcomas and to clarify which MRI features best indicate tumors with adverse clinical behavior.

MATERIALS AND METHODS. The initial MRI studies of 36 pathologically confirmed myxoid–round cell liposarcomas were retrospectively reviewed, and observations from this review were correlated with the histopathologic features. MR images were evaluated by two radiologists with agreement by consensus, and both univariate and multivariate analyses were conducted to evaluate survival with a median clinical follow-up of 33 months (range, 9–276 months).

RESULTS. Statistically significant MRI findings that favored a diagnosis of intermediate- or high-grade tumor were large tumor size (> 10 cm), deeply situated tumor, tumor possessing irregular contours, absence of lobulation, absence of thin septa, presence of thick septa, absence of tumor capsule, high-intensity signal pattern, pronounced enhancement, and globular or nodular enhancement. Of these MRI findings, thin septa ($p < 0.05$), a tumor capsule ($p < 0.01$), and pronounced enhancement ($p < 0.01$) were associated significantly, according to univariate analysis, with overall survival. Multivariate analysis indicated that pronounced enhancement was associated significantly with overall survival ($p < 0.05$).

CONCLUSION. Contrast-enhanced MRI findings can indicate a good or adverse prognosis in patients with myxoid–round cell liposarcomas.

Liposarcomas are classified into well-differentiated, myxoid, round cell, and pleomorphic subtypes. Myxoid liposarcomas are the most common subtype of liposarcoma, occurring in the extremities of adults. They are considered low-grade sarcomas with a low risk of metastasis and are associated with prolonged survival [1–5]. On the other hand, round cell liposarcomas are considered high-grade sarcomas with a higher likelihood of metastasis and mortality due to disease [1–5]. Recent studies reveal that myxoid and round cell liposarcomas belong to a continuous histopathologic spectrum characterized by a chromosome translocation t(12;16)(q13;p11) resulting in the fusion transcript of the *TLS* and *CHOP* genes [6–9]. However, diagnosis and prognostic predictions can often be complicated by lesions that contain admixed morphologic components of myxoid and round cell subtypes.

The characteristic MRI features of myxoid–round cell liposarcomas are attributable to the predominantly myxoid matrix of the tumor. Tumors appear on T2-weighted MR images as encapsulated tumors with signals that are hyperintense compared with the surrounding structures [10–14]. On contrast-enhanced studies, they often show marked or heterogeneous enhancement with nonenhanced areas corresponding to myxoid material [13, 14]. As expected from the fact that the histopathologic spectrum from myxoid to round cell liposarcomas is continuous, these tumors show considerable diversity on imaging. Therefore, it is important to review the reliability of MRI features for characterizing myxoid–round cell liposarcomas. The objectives of this study were to determine the prognostic significance of MRI findings in patients with myxoid–round cell liposarcomas and to clarify which MRI features best indicate tumors with adverse clinical behavior.

Received February 3, 2003; accepted after revision July 11, 2003.

[1]Division of Diagnostic Radiology, National Cancer Center Hospital and Research Institute, Tsukiji, Chuo-Ku, Tokyo 104-0045, Japan. Address correspondence to U. Tateishi.

[2]Division of Pathology, National Cancer Center Hospital and Research Institute, Tsukiji, Chuo-Ku, Tokyo 104-0045, Japan.

[3]Division of Orthopedics, National Cancer Center Hospital and Research Institute, Tsukiji, Chuo-Ku, Tokyo 104-0045, Japan.

AJR 2004;182:725–731

0361–803X/04/1823–725

Materials and Methods

Patients

We reviewed materials from 36 patients with myxoid–round cell liposarcomas, all of whom who were registered in our pathology files. The clinical details, including follow-up information, were obtained by reviewing all the medical charts. None of the patients was lost to follow-up, which began on the date of primary surgery. The median duration of follow-up was 33 months and ranged from 9 to 276 months. The time to death due to any cause was recorded to determine the overall survival rate.

MRI Studies and Pathologic Correlations

MRI was performed using one of two 1.5-T systems (Horizon, General Electric Medical Systems, Milwaukee, WI; or Visart, Toshiba Medical Systems, Tokyo, Japan). Either the spin-echo or the fast spin-echo technique was used to obtain T1-weighted images (TR range/TE range, 460–720/12–27) in one or more planes (coronal or axial). T2-weighted images (TR range/TE_{eff} range, 3,500–6,000/96–112; echo-train length, 8–12) with flow compensation and presaturation superiorly and inferiorly were then obtained in one or more planes using a body coil. The images were obtained with a field of view of 30–40 cm, an image matrix of 128 × 256, and a slice thickness of 6–10 mm. Gadopentetate dimeglumine was administered IV, and T1-weighted images were obtained in one or more planes with (n = 20) or without (n = 16) fat suppression.

Two radiologists reviewed the MR images, and the findings were reported as a consensus opinion. The lesions were judged according to size, location, depth (superficial or deep), type of margin and contours, internal architecture, presence of a tumor capsule, signal characteristics on T1- and T2-weighted images, and homogeneity (homogeneous or heterogeneous). A superficial tumor (dermal or subcutaneous tumor) was located exclusively above the superficial fascia without invasion of the fascia, whereas a deep tumor was located either exclusively beneath the superficial fascia or superficial to the fascia with invasion of or through the fascia. The signal characteristics were described as isointense or hyperintense relative to the signal intensity of skeletal muscle. The extent (none and weak or pronounced), pattern (globular and nodular or diffuse), and homogeneity of gadolinium-based enhancement were also recorded. Globular and nodular enhancement corresponded to spotty enhancement (range, 3–10 mm) within the mass on contrast-enhanced MR images. Septal structures were categorized as thin (uniform linear structures ≤ 2 mm) or thick (focally thickened linear structures > 2 mm). Tumors containing areas with high-intensity characteristics on both T1- and T2-weighted MR images were considered positive for a high-intensity signal pattern.

Histologic slides of all the patients' tumors were reviewed for diagnosis by an expert pathologist. Immunohistochemical staining was performed in all cases to confirm the diagnosis or tumor type according to the classification system described by Enzinger and Weiss [1]. In this study, the histologic grade of a tumor was determined using a three-grade system established by Hasegawa et al. [15–17]. According to this system, myxoid–round cell liposarcomas are assigned a grade of 1, 2, or 3. Grade 1 tumors (n = 12, 33.3%) are considered low-grade tumors, grade 2 tumors (n = 14, 38.9%) are intermediate-grade tumors, and grade 3 tumors (n = 10, 27.8%) are high-grade tumors (n = 24, 66.7%). Excised specimens were available for review or for mapping correlation with images. Pathology reports were reviewed for descriptive comments characterizing the necrosis and myxoid–round cell tumor components of the lesions.

Statistical Analysis

Patients' demographics and imaging characteristics were compared using Wilcoxon's rank sum test for continuous variables and the chi-square test or Fisher's exact test for categorized variables. Univariate analysis was performed by comparing survival curves generated using the Kaplan-Meier method and carrying out log-rank tests. The relative risk of each variable subjected to multivariate analysis was estimated using a Cox proportional hazards model. All analyses were conducted using SPSS software version 11.0J (Statistical Package for the Social Sciences, Chicago, IL) for Windows (Microsoft, Redmond, WA). Differences and correlations at a p value of less than 0.05 were considered statistically significant.

Results

Twenty-one (58.3%) of the 36 patients were men and 15 were women (41.7%). The mean age at diagnosis was 47 years, and the patients ranged in age from 17 to 87 years. The tumors were located on the lower extremities in 31 patients (86.1%) and the trunk in five (13.9%). The mean tumor size was 9.6 cm, and 16 tumors (44.4%) were larger than 10 cm. Thirty-one tumors (86.1%) were situated deeply, and five (13.9%) were superficial. The surgical procedures consisted of wide excision, amputation, or disarticulation. Surgical margins were confirmed to be adequate at pathology in 28 patients (77.8%). Marginal or intralesional excision with inadequate margins were found in eight (22.2%). Additional treatment included chemotherapy in five patients (13.9%), radiotherapy in nine (25.0%), and both in seven (19.4%).

Metastases occurred in 11 (30.6%) of the 36 patients; the location of metastasis was the peritoneal cavity in five patients (13.9%), soft-tissue in five (13.9%), lung in three (8.3%), and bone, liver, retroperitoneum, and mediastinum in one (2.8%). Eight (38.0%) of the 21 patients who received additional treatment had metastasis subsequently. Twelve (33.3%) of the 36 patients developed local recurrences. Three patients (8.3%) with inadequate excision had local recurrence. Four patients (11.1%) with local recurrence underwent additional therapy.

Ten (27.8%) and 26 (72.2%) of 36 tumors had regular and irregular tumor contours, respectively (Figs. 1–4). Sixteen tumors (44.4%) showed lob-

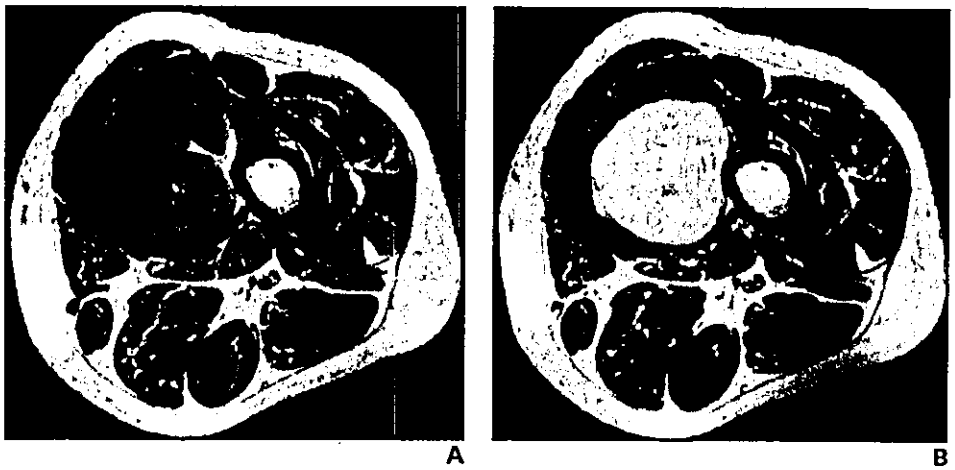

Fig. 1.—38-year-old woman with low-grade myxoid–round cell liposarcoma in left thigh.
A, T1-weighted spin-echo MR image (TR/TE, 720/20) shows tumor has regular contours with small amount of fat signal in periphery (*arrowhead*).
B, Contrast-enhanced T1-weighted spin-echo MR image (720/20) shows diffuse enhancement of tumor.

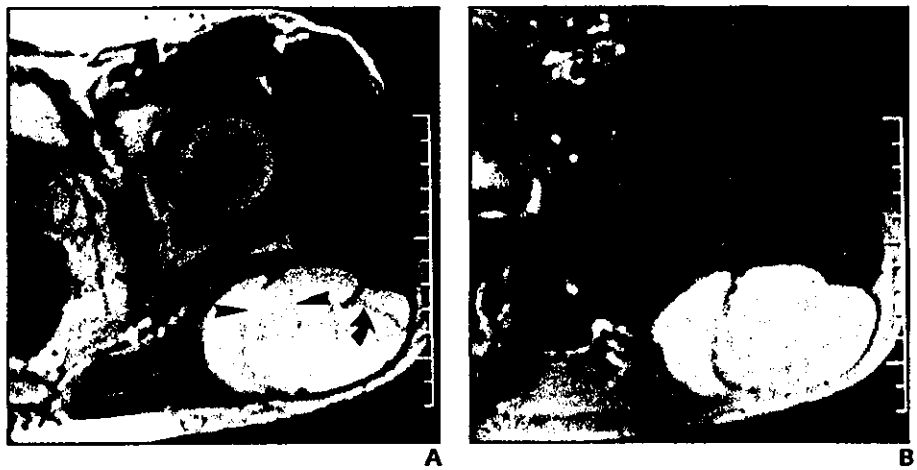

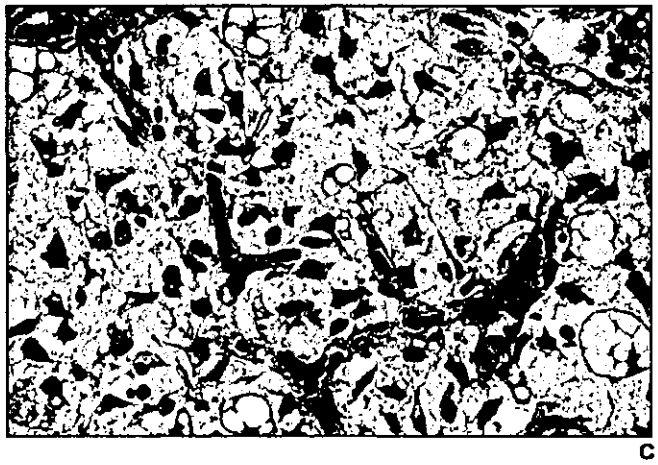

Fig. 2.—62-year-old man with low-grade myxoid–round cell liposarcoma in left buttock.
A, Axial T2-weighted fast spin-echo MR image (TR/TE, 3,500/100) shows septate appearance of lesion. Linear structures of low intensity contained thick septa (*arrow*) and thin septa (*arrowheads*).
B, Axial fat-saturated contrast-enhanced T1-weighted spin-echo MR image (720/20) shows tumor of high intensity with slight enhancement of septa.
C, Photomicrograph of specimen shows paucicellular myxoid liposarcoma with less than 25% round cell components has dispersed small round or short spindled cells and multivacuolated lipoblasts within abundant myxoid matrix and plexiform vascular network. (H and E, ×200)

ulated morphology. On MR images, thin and thick septa (Fig. 2) were identified in 31 (86.1%) and 10 (27.8%) tumors, respectively. On T1-weighted MR images the signals of the tumors relative to those of muscle were hyperintense ($n = 15$), isointense ($n = 12$), or hypointense ($n = 9$). Tumors showed predominantly increased signal intensity compared with that of the skeletal muscle on T2-weighted MR images. The images showed the tumor as having a heterogeneous appearance with thin or thick septa of low intensity. High-intensity signals similar to subcutaneous fatty tissue (high-intensity signal pattern) were found in 15 tumors (41.7%) on both T1- and T2-weighted MR images (Figs. 1 and 4).

On contrast-enhanced MR images, pronounced enhancement (Fig. 4) located mostly at the peripheries of the lesions was present in 22 tumors (61.1%). Globular and nodular enhancement (Figs. 3 and 4) was found mostly in the centers of the lesions of 16 patients (44.4%), whereas diffuse enhancement (Fig. 1) was seen in six lesions (16.7%). Contrast-enhanced MR images also revealed that 23 tumors (63.9%) had homogeneously enhanced tumor capsules (Fig. 3).

All tumors were characterized microscopically by a prominent plexiform vascular pattern admixed with an abundant myxoid matrix. The extent of cellularity ranged from slight to moderate, and the lesions were composed of small uniform, round, or spindle-shaped hyperchromatic cells. Tumor necrosis was found on microscopic observation in 12 cases (33.3%). The necrotic areas varied in degree, but most tumors contained only a small amount of necrotic areas that were difficult to identify on MR images.

Statistically significant MRI findings that favored a diagnosis of intermediate- or high-grade tumor were large tumor size (> 10 cm) ($p < 0.01$), deeply situated tumor ($p < 0.05$), tumor possessing irregular contours ($p < 0.001$), absence of lobulation ($p < 0.001$), absence of thin septa ($p < 0.05$), presence of thick septa ($p < 0.01$), absence of tumor capsule ($p < 0.001$), high-intensity signal pattern ($p < 0.01$), pronounced enhancement ($p < 0.001$), and globular and nodular enhancement ($p < 0.001$). The presence of thin septa or a tumor capsule indicates low-grade tumor. Irregular contours were found in only 10 high-grade tumors (58.8%). All the low-grade tumors had a capsule, thin septa, and a high-intensity signal pattern. The odds ratios for a specific finding favoring a diagnosis of intermediate- or high-grade tumor are shown in Table 1. The multiple logistic regression model showed that irregular contour and thick septa were the most significant predictors of intermediate- or high-grade tumors, with an odds ratio of 13.8 for both (95% confidence interval [CI], 1.5–128.8; $p < 0.05$).

At the last follow-up, 10 (27.8%) of the 36 patients had died of their disease and four (11.1%) were alive with metastatic disease. The 5- and 10-year survival rates were 80.5%

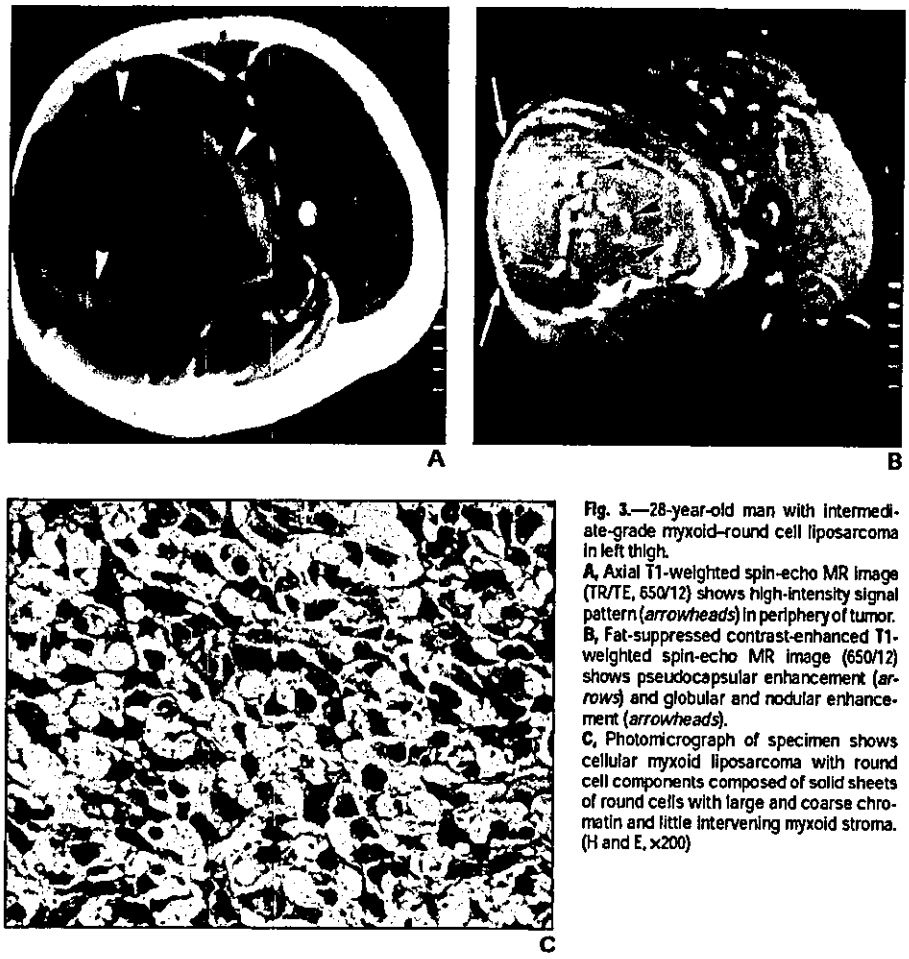

Fig. 3.—28-year-old man with intermediate-grade myxoid–round cell liposarcoma in left thigh.
A, Axial T1-weighted spin-echo MR image (TR/TE, 650/12) shows high-intensity signal pattern (*arrowheads*) in periphery of tumor.
B, Fat-suppressed contrast-enhanced T1-weighted spin-echo MR image (650/12) shows pseudocapsular enhancement (*arrows*) and globular and nodular enhancement (*arrowheads*).
C, Photomicrograph of specimen shows cellular myxoid liposarcoma with round cell components composed of solid sheets of round cells with large and coarse chromatin and little intervening myxoid stroma. (H and E, ×200)

and 72.4%, respectively. The univariate analysis showed that thin septa ($p < 0.05$), tumor capsule ($p < 0.01$), and pronounced enhancement ($p < 0.01$) were significantly associated with overall survival (Table 2). The multivariate analysis revealed that pronounced enhancement was the most significant adverse prognostic factor (Fig. 5) with a relative risk of 7.3 (95% CI, 1.5–35.1; $p < 0.05$).

TABLE 1: Odds Ratio for Features Favoring Diagnosis of Intermediate- or High-Grade Myxoid–Round Cell Liposarcoma

Feature	Odds Ratio	95% CI
Size > 10 cm	9.0	2.6–30.9
Lobulation absent	21.0	8.3–126.5
Thick septa present	20.3	2.1–188.7
Pronounced enhancement present	34.7	3.72–324.1
Globular and nodular enhancement present	9.0	2.0–41.3

Note.—CI = confidence interval.

Discussion

In this study, we documented the prognostic significance of MRI features in patients with myxoid–round cell liposarcomas. Univariate analysis revealed that the presence of thin septa, a tumor capsule, and pronounced enhancement had a significant correlation with overall survival. Multivariate analysis showed that, of these variables, pronounced enhancement on contrast-enhanced MR images was the most influential adverse prognostic factor. This MRI finding of enhancement correlated with the round cell–component content on pathologic specimens. The prognostic importance of the round cell component has been acknowledged in previous studies [18–20]. From a practical viewpoint, detection of this enhancement pattern on contrast-enhanced MR images in myxoid–round cell liposarcomas is useful for predicting their behavior.

The amount of necrosis has been reported to be correlated with clinical outcome [21–25]. Spontaneous tumor necrosis identified in four (4%) of 95 patients with myxoid–round cell liposarcomas was correlated with increased risks of metastasis and death [18]. In our study, we did not evaluate the relationship between the presence of tumor necrosis and patient prognosis, because most tumors accompanied by necrosis in our study contained only a small amount of necrotic areas that were difficult to identify on MR images.

On contrast-enhanced MR images, pronounced enhancement was located mainly at the periphery of the lesion in 61.1% of the pa-

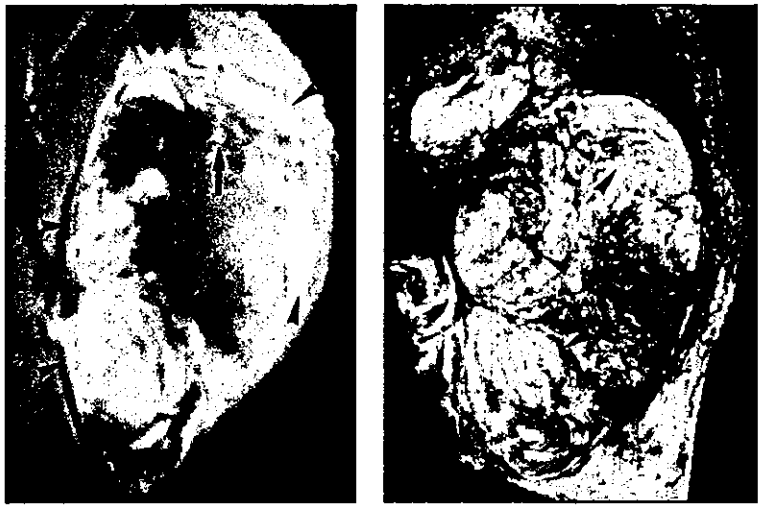

A B

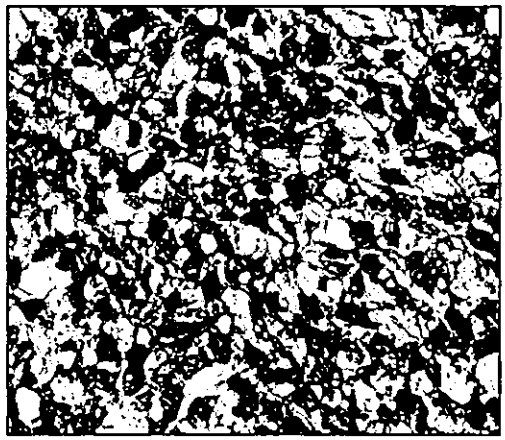

C

Fig. 4.—69-year-old man with high-grade myxoid–round cell liposarcoma in left thigh.
A, Sagittal contrast-enhanced T1-weighted spin-echo MR image (TR/TE, 600/15) shows globular and nodular enhancement (*arrows*) and pronounced enhancement (*arrowheads*) predominantly at tumor periphery.
B, Photograph of macroscopic specimen of same tumor as in A shows heterogeneous tumor components (*arrowheads*).
C, Photomicrograph shows that specimen is composed of solid sheets of uniform round cells with large and coarse chromatin. (H and E, ×200)

tients, and globular and nodular enhancement occurred at the lesion center in 44.4%. These two patterns of enhancement were characteristic of intermediate- or high-grade tumors. Round cell components were reported to be located at the peripheries of lobules; adjacent to fibrous septa extending through the tumor; and surrounding large vessels, particularly in tumors with only a small amount of round cell components [7, 8]. Thus, these two enhancement patterns may be reliable imaging findings for detecting round cell components within tumors. In one study, despite a small sample size, researchers showed that patients (n = 5) who initially had a tumor with 5% or greater round cell components had a significantly higher incidence of metastasis or death from disease than those (n = 7) who initially had a tumor with less than 5% round cell components [18]. In a study of 24 patients with round cell components composing 25% or more of the tumor, round cell components were associated significantly with a lower survival rate [19]. However, the correlation between the quantity of round cell components and the clinical outcome may depend on the difficulty in quantifying the round cell components at transitional areas at microscopic observation.

There was no significant difference between the risks of an adverse outcome in patients with myxoid and transitional areas without round cell components and those with myxoid areas alone [19]. The pathologic variables responsible for differences among observers in identifying round cell components are considered to be numerous and include inaccurate criteria for tissue processing and selection of the assessment area within the spectrum of myxoid–round cell liposarcomas [20]. Our results suggest that contrast-enhanced MR images can assist in detecting round cell component content within the entire tumor and assist in the distinction of low-grade and of intermediate- or high-grade myxoid–round cell liposarcomas.

In previous reports [26–29], the descriptions of the enhancement patterns identified on MR images included little enhancement or a few patterns (i.e., heterogeneous, homogeneous, no enhancement). However, the end points selected in these prior studies depended simply on the pathologic diagnosis of "myxoid liposarcoma," and the investigators were unaware of the lineage of "myxoid–round cell liposarcoma" as a disease entity. The results of our study are based on a definite diagnosis of myxoid–round cell liposarcoma, and we stress that

TABLE 2 MRI Findings and Univariate Analyses of Survival in 36 Cases of Myxoid–Round Cell Liposarcoma

MRI Findings	No. (%) of Cases	5-Year Survival Rate (%)	p^a
Size (cm)			0.10
≤ 10	20 (55.6)	84.2	
> 10	16 (44.4)	56.8	
Depth			0.26
Superficial	5 (13.9)	100	
Deep	31 (86.1)	66.7	
Contour			0.27
Regular	26 (72.2)	71.2	
Irregular	10 (27.8)	62.5	
Lobulation			0.19
Absent	20 (55.6)	59.8	
Present	16 (44.4)	85.2	
Thin septa			0.02
Absent	5 (13.9)	26.7	
Present	31 (86.1)	77.1	
Thick septa			0.47
Absent	26 (72.2)	66.7	
Present	10 (27.8)	72.3	
Tumor capsule			< 0.01
Absent	13 (36.1)	16.6	
Present	23 (63.9)	83.1	
Pronounced enhancement			< 0.01
Absent	14 (38.9)	100	
Present	22 (61.1)	54.9	
Globular and nodular enhancement			0.91
Absent	20 (55.6)	78.4	
Present	16 (44.4)	66.8	
High-intensity signal pattern			0.71
Absent	21 (58.3)	72.4	
Present	15 (41.7)	69.1	

[a]Log-rank test.

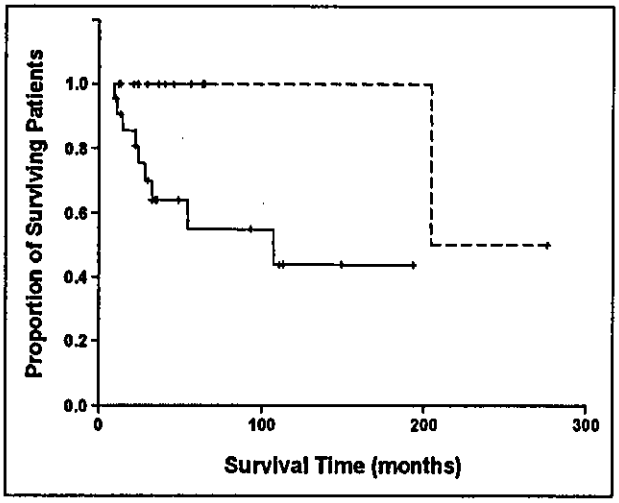

Fig. 5.—Graph shows Kaplan-Meier survival curve according to presence (*solid line*) or absence (*dashed line*) of pronounced enhancement on contrast-enhanced MR images for 36 patients with myxoid–round cell liposarcomas.

the presence of globular and nodular or pronounced enhancement identified on MRI is a finding suggestive of intermediate- or high-grade tumor and reflects the amount of round cell components in the tumor, which strongly affects patient outcome.

The presence of linear or amorphous hyperintense foci behaving like fatty tissue on T1-weighted MR images has been reported to be a pattern suggestive of myxoid liposarcoma [27]. Myxoid–round cell liposarcoma often consists of multiple histologic subtypes in the same lesion. We observed a high-intensity signal pattern in 15 low-grade tumors, and this finding was consistent with immature fatty tissue or the fat components of the tumors. Immature spindle cells lacking obvious fat genesis may be seen next to multivacuolated lipoblasts. Although MRI is sensitive enough to detect minute fat deposits or immature fatty components, our univariate analysis showed no significant association between high-intensity signal pattern on MR images and survival [28, 29].

In summary, the spectrum of MRI findings in myxoid–round cell liposarcomas is continuous. MRI findings can assist in the distinction between low-grade and intermediate- or high-grade myxoid–round cell liposarcomas. MRI findings that favored a diagnosis of intermediate- or high-grade tumor included large (> 10 cm) size of tumor, deeply situated tumor, tumor possessing irregular contours, absence of lobulation, absence of a tumor capsule, absence of thin septa, presence of thick septa, high-intensity signal pattern, pronounced enhancement, and globular and nodular enhancement. The presence of thin septa or a tumor capsule indicates low-grade tumor. Imaging features associated with overall survival were thin septa, a tumor capsule, and pronounced enhancement. Multivariate analysis showed that pronounced enhancement on MRI is the most significant factor in predicting an adverse prognosis for patients with myxoid–round cell liposarcoma.

References

1. Enzinger FM, Weiss SW. *Soft tissue tumors*, 4th ed. St. Louis, MO: Mosby–Year Book, 2001: 670–687
2. Enzinger FM, Winslow DJ. Liposarcoma: a study of 103 cases [in German]. *Virchows Arch Path Anat Physiol Klin Med* 1962;335:367–388
3. Evans HL. Liposarcoma: a study of 55 cases with a reassessment of its classification. *Am J Surg Pathol* 1979;3:507–523
4. Evans HL. Liposarcomas and atypical lipomatous tumors: a study of 66 cases followed for a minimum of 10 years. *Surg Pathol* 1988;1:41–54